minerals

MDPI

Article

Advances in Glendonite Understanding and Its Potential for Carbon Capture

Bo Pagh Schultz [1,*] and Jennifer Huggett [2]

[1] Museum Salling, Fur Museum, Nederby 28, 7884 Fur, Denmark
[2] The Natural History Museum, Cromwell Road, London SW7 5BD, UK; jmhuggett@icloud.com
* Correspondence: bosc@museumsalling.dk

Abstract: This article reviews recent advances made by the authors through evaluation of samples in museum collections, in the context of our recent advances in novel observations, of cleavage in a recrystallising ikaite crystal, that may guide future research in understanding the morphology of ikaite, which traditional crystallography has so far not achieved, as traditional crystallography cannot be applied to the morphology of ikaite. Having reviewed over 1100 samples in museum collections, using a combination of morphology and petrology, we are able to define how samples can be classified as glendonite. The topics covered include: (1) a historical review of ikaite and glendonite; (2) evidence supporting ikaite as the precursor mineral of glendonite; (3) the discovery of mega-sized Danish glendonites; and (4) Holocene glendonite coastal sites. Our reassessment of existing knowledge of ikaite shows that when ikaite forms in marine settings, it forms in specific zones before other carbonate phases, and that in sedimentary environments, pressure and pH are not the primary factors controlling its precipitation. Instead, the availability of magnesium (Mg^{2+}) and phosphate (PO_4^{3-}) ions appear to play a more significant role. Furthermore, the conditions required for ikaite precipitation in laboratory experiments differ from those observed in natural ikaite or glendonite formation. Ikaite's ability to capture carbon at low temperatures and its rapid recrystallisation into its more stable calcite pseudomorph, glendonite, suggest a potential application in carbon capture strategies.

Keywords: ikaite; glendonite

check for updates

Academic Editors: Gabrielle J. Stockmann and Juan Diego Rodríguez-Blanco

Received: 24 February 2025
Revised: 2 April 2025
Accepted: 3 April 2025
Published: 13 April 2025

Citation: Schultz, B.P.; Huggett, J. Advances in Glendonite Understanding and Its Potential for Carbon Capture. *Minerals* **2025**, *15*, 410. https://doi.org/10.3390/min15040410

Copyright: © 2025 by the authors. Licensee MDPI, Basel, Switzerland. This article is an open access article distributed under the terms and conditions of the Creative Commons Attribution (CC BY) license (https://creativecommons.org/licenses/by/4.0/).

1. Introduction

The present special issue on ikaite ($CaCO_3 * 6H_2O$) and glendonite provides a platform for presenting a synthesis by the first author of 30 years of work on that topic, only made possible by significant help from various international colleagues [1]. Our dear colleague Erwin Suess, who died in 2023, advised us to gather and present as much information as possible, to resolve the enigma of how ikaite can be abundant over a limited lateral extent and a restricted time interval, named here Ikaite Forming Zones (IFZ). Many of our previous papers, supported by other recent publications, address this issue (Figures 4, 5 and 6) and provide data for new geological sites, as well as sites that have played a significant historical role in the glendonite/ikaite research, (see Tables S1 and S2 in Supplementary Materials).

Over 650 ikaite and glendonite sites are collated in Rogov et al. [2], together with full references and paleogeographic maps. Extensive though the data set in Rogov et al. [2] is, it includes little morphological data. In this article we consider the morphology and petrology of samples from Fur Museum, Denmark (680 samples), the Fossil and Mo Clay Museum of Mors, Denmark (265 samples), the Natural History Museum London, UK

(120 samples), the Mineralogies Museum in Hamburg, Germany (65 samples), and the Museum of Natural History in Copenhagen, Denmark (55 samples). This totals over 1100 catalogued samples from 27 different localities, settings, and time periods. All the samples share key morphological points [1,3–6] and guttulatic petrology [7]. We use an updated version of glendonite classification by morphology and petrology, based on that of Frank et al. [8]. Crystallographic identification alone is insufficient, due to crystallographic distortions [9]; morphology and petrography also need to be considered [4,5]. Detailed observation of the ikaite to calcite transformation [10] forms the basis for our method of identification of ikaite as the precursor mineral to glendonites [5]. In Ref. [6] we have applied this method to a number of historic sites, now only known from publications and museum collections. Images and size data are provided in Supplementary Material S1, and morphological, petrographic and settings detail in Supplementary Table S1.

Ikaite has been described as a rogue mineral, difficult to understand. The enigma of what makes ikaite form in sediment is still not fully understood; for instance, mega-size glendonites in Denmark are found just after the Palaeocene Eocene Thermal Maximum, hence corresponding to a hothouse climate mode, contrasting with the primarily polar and/or cold-water settings of IFZs today. The finding of glendonites in the Mid-Norwegian margin under the hothouse climate mode of the late Paleocene to early Eocene transition reinforces this enigma, much in contradiction with the known common environmental conditions for the formation of ikaite [11]. A further problem is determining the factors that inhibit the crystallisation of calcite, and favour crystallisation of ikaite in various depositional settings. The purpose of this paper is thus to illustrate these aspects as well as to review the range of various consistent morphologies, petrological and geochemical aspects of ikaite and glendonite across a wide range of geological locations. Our review mainly revolves around a set of papers published by our team in the past five years. In recognition of the historical importance of both the mineral ikaite and its pseudo-morph glendonite [1,2] we show in Figure 1 significant images not previously presented.

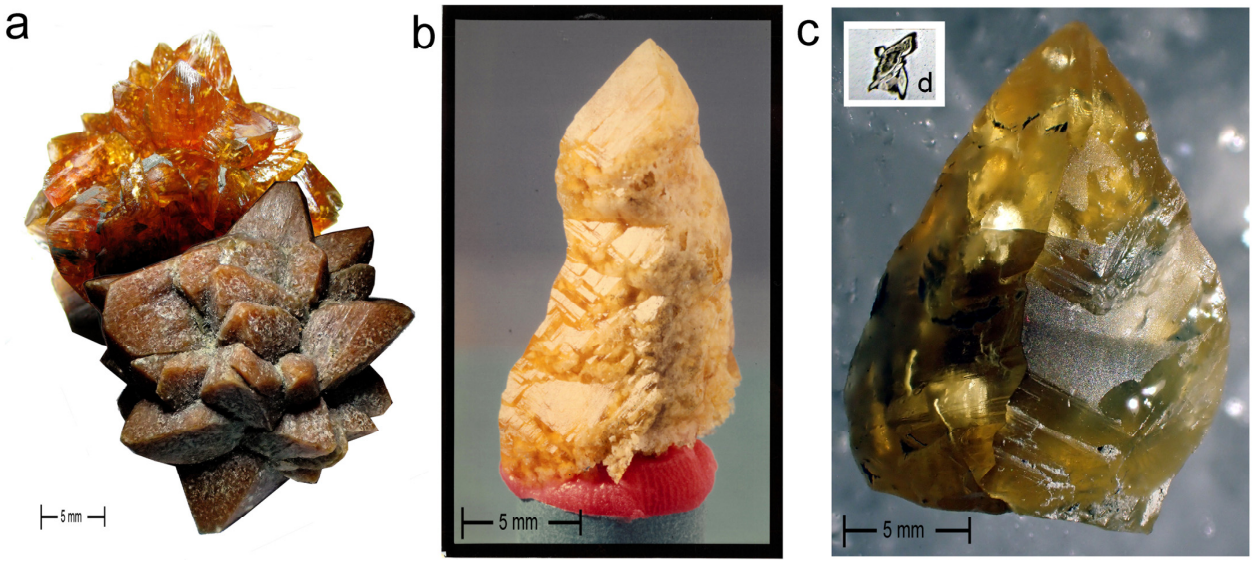


Figure 1. *Cont.*

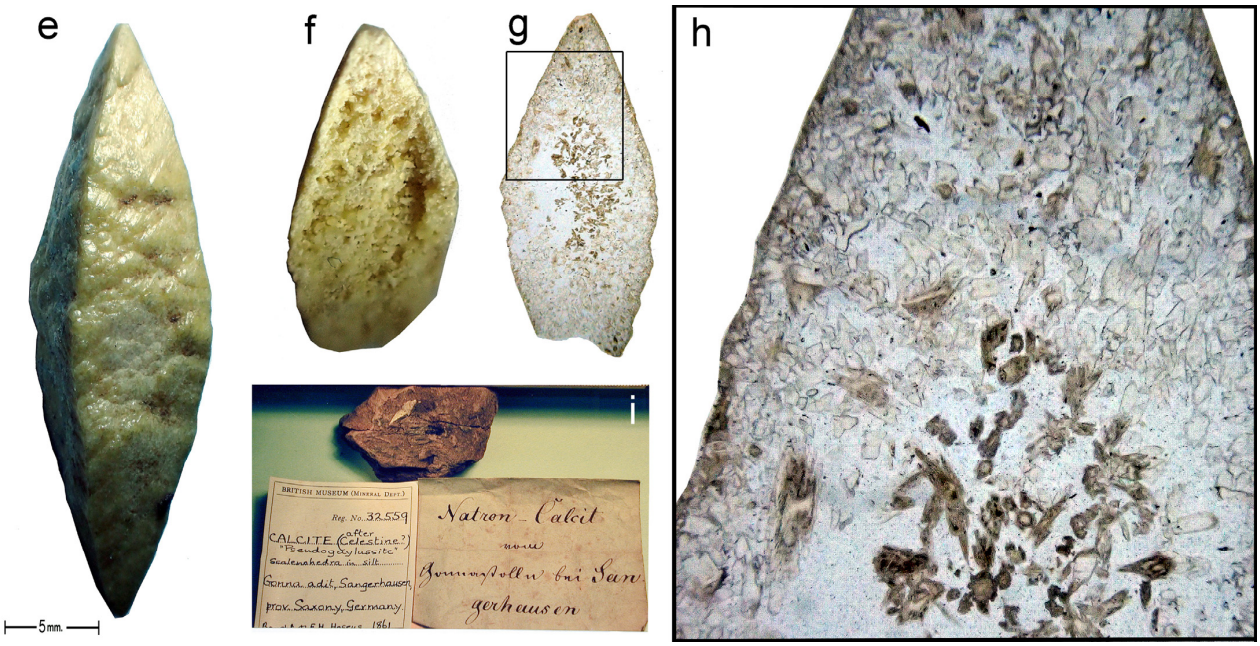


Figure 1. Images of emblematic ikaite and glendonite crystals: (**a**) is a collage, showing a glendonite from Olenitsa, Russia, in front, and a Laptev Sea ikaite behind [12] (photograph by A.A. Krylov). Note the similarity in the morphology of the two distinct crystals. (**b**) is the Bransfield ikaite captured by Erwin Suess in haste as he realised the mineral was crumbling. The image hard copy came to Douglas Shearman from whom Bo Schultz got it in 1994. It is from the same Ikaite Formation Zone as the crystal depicted in [13] (photo Erwin Suess). (**c**) The ikaite crystal (GC-16, GeoB 22049-3) collected by Bohrmann at South Georgia in 2017 [14]. (**d**) is a guttulatic 1 mm-large calcite grain generated when the ikaite crystal recrystallised [5,10]. (**e**) Sangerhausen glendonite originally presented as pseudogaylussite or barlycorn. (**f**) A Sangerhausen, (**g**) cut open to show the porous matrix of small crystals, (**h**) as a thin section, and (**h**) enlarged so the guttulatic grains can be shown. (**i**) A sample from the Natural History Museum London, where the crystal is in situ in clay.

The excellent preservation and the various morphologies of giant-sized Early Eocene "mega"-glendonites present in specific strata of the Fur Formation, a fossil-rich tephra-bearing marine diatomite from the Danish Eocene, have been previously described [3]. In addition, we briefly presented other Danish glendonites originating from the Late Oligocene Brejning Formation. In ref. [3] we also briefly reviewed conditions of naturally occurring ikaite, introduced the concept of Ikaite Formation Zones, and discussed the relationship between the precursor ikaite and its glendonite pseudomorph. Using clumped isotope analysis, Vickers et al. [15] demonstrated that the Danish Eocene mega-glendonites crystallised at bottom-water temperatures <5 °C, suggestive of a post Paleocene/Eocene Thermal Maximum (PETM) cooling episode that may have been linked to the release of sulphate aerosols from eruptive phases of the North Atlantic Igneous Province. This hypothesis has been reinforced [1], showing that the Danish mega-glendonites cluster in restricted stratigraphic intervals of the Fur Formation that coincide with minima in sea-surface temperatures, as recorded through a compilation of recently published Tex86 values. In reference [1] the historical context of the discovery of ikaite was reviewed, and the progressive link made to its glendonite pseudomorphs and the various names previously attributed to this mineral. We reviewed the potential conditions leading to the formation of ikaite, as well as the use of glendonites in the literature as paleoenvironmental indicators of near-freezing temperatures. Ref. applied a series of similar isotopic, elemental, and SEM analysis to both air-dried transformed ikaite samples from Point Barrow, Alaska, and recent glendonites from the White Sea, Russia. These findings reinforced the link

between ikaite and glendonite, showing that at room temperature, the ikaite to calcite transformation occurs through a coupled dissolution-reprecipitation mechanism as ikaite progressively loses water, while the parent mineral and its pseudomorph show similar petrology at both macroscopic and microscopic scales [4]. In contrast, Vickers et al. [10] found that ikaite undergoes a quasi-solid state transformation to calcite upon heating, with limited dissolution-recrystallisation. Also, the latter study showed that Mg incorporation into the ikaite structure reduces its stability and that bacterial sulphate reduction and methanogenesis or anaerobic oxidation of methane intervene in the formation of ikaite. The morphology and petrology of ikaite have been further investigated, through the inclusion of recrystallised ikaite samples from four additional polar and/or deep-sea localities (Figure 2), demonstrating that glendonite petrographic characteristics result primarily from the original structure and chemistry of recrystallising ikaite and not from external environmental factors. [5]. Recent coastal Holocene glendonites from various locations have been studied to establish a more accurate chronology of these occurrences through radiocarbon dating [6]. The study also highlighted a fundamental flaw in our understanding of Ikaite Formation Zones, namely that glendonite pseudomorphs can be abundant in specific areas but absent in adjacent areas with very similar environmental, physical, and chemical conditions.

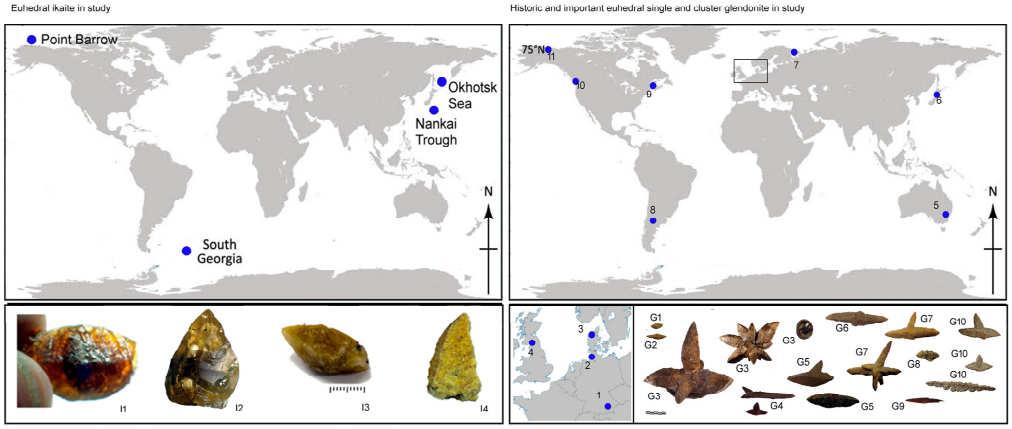


Figure 2. The sites and samples. Panel A focuses on published examples of Ikaite. (**I1**) Point Barrow [16], (**I2**) South Georgia [14], (**I3**) Nankai Trough [17], (**I4**) Okhotsk Sea [18]. Panel B focuses on recently published examples of glendonites coming from the following localities: (**G1**) Sangerhausen in Germany [1]. (**G2**) Tonningen in Germany [6]. (**G3**) Early Eocene and late Oligocene in Denmark [3]. (**G4**) River Clyde [6]. (**G5**) NSW in Australia [8]. (**G6**) Hokkaido in Japan [19]. (**G7**) White Sea in Russia [20,21]. (**G8**) Patagonia in Argentina [22]. (**G9**) Fundy in Canada [23]. (**G10**) Olympic Peninsula in Washington State, USA [24]. References and data are listed in Supplementary Materials, Tables S1 and S2). For more information on the history of ikaite and glendonite see ref. [1].

2. Study Sites

From the excellent compilation [2] reviewing ca. 900 occurrences of either ikaite or glendonite, it appears the mineral ikaite occurs in a very broad range of environments but is somewhat restricted to polar and/or deep cool water settings [1,2], while glendonite occurrences in the geological record appear to match geochemical environments consistent with ikaite precipitation [13]. For the past 60 years following the first discovery of ikaite, geologists have debated the relationship between the metastable ikaite mineral ($CaCO_3$ * $6H_2O$), and the calcific glendonites, found in many intervals of the Phanerozoic sedimentary record [2]. In recent studies, we have striven to unequivocally link ikaite to glendonite, through studies of their morphology and petrography. Our dataset derives from many sites from which we could obtain samples (Figure 1). While it is way more limited than the extensive review of sites in ref. [2], we have, however, described and analysed in total

material originating from no less than 30 distinct glendonite sites, and nine recent/Holocene ikaite sites (Figure 2), which have played central roles in the ongoing unravelling of the ikaite enigma and its relationship to glendonite [1,16]. With regard to glendonite, we mainly review here the morphology and petrology discussed in previous publications [1,3–6], but also include new observations from historical sites: Sangerhausen in Germany [1,25], Patagonia [22], and Codroy on Newfoundland [23]. Another interesting shared feature observed in glendonites from various locations seems to be the presence of secondary parasitic growth, as observed in glendonites from the river Clyde (Holocene, Scotland) [6], Silstrup (late Oligocene, Denmark) [3], and Cater Creek (late Oligocene, Alaska) [26].

3. Methods

Three-D scanning and image stacking of glendonite and ikaite crystals were performed using an ATOS Core 80 sensor at Zebicon, Billund, Denmark. Details were extracted using the GOM Inspect 2017 program. Image stacking was performed using an Olympus TG4 camera. Petrographic images were captured using a Zeiss petrographic microscope with digital camera.

Scanning Electron Microscopy with Energy Dispersive Spectroscopy (EDS) and Backscatter Scanning Electron Imaging (BSEI) were used to examine carbon-coated polished thin-sections of recrystallised Utqiaġvik ikaite at Aarhus University with an Electron microprobe JEOLJXA-8600 at 15–20 kV and a 1 nA beam. Elements analysed were Ca, Mg, Mn, Fe, and Sr as incorporated in the lattice of calcite.

A Tescan Mira3 High Resolution Schottky Field Emission (FEG-SEM) fitted with both standard and in-lens secondary electron, as well as back-scattered electron detectors was used at Lund University to observe ikaite transformation into calcite in order to further constrain the nature of this transformation. For this purpose, uncoated samples of ikaite, taken from the freezer, were mounted on stubs at ambient temperature (c. 21 °C) and were examined in the SEM under low vacuum mode at a pressure of 60 Pa, with no additional temperature regulation. The acceleration voltage was set to 15 kV and the working distance varied between 5 and 15 mm.

4. Linking Ikaite to Glendonite

Geologists have long wondered about the relationship between the metastable ikaite mineral found today in various polar and cool-water environments, such as the famous Ikka Fjord in Greenland, and the calcitic glendonites, found in many intervals of the Phanerozoic sedimentary record. Although the Ikka Fjord's large, sub-merged ikaite tufa pillars bear no resemblance to glendonite, large yellow/orange euhedral ikaite crystals resembling glendonite morphology were first found in the Bransfield Strait, offshore Antarctica [27]. A historical summary of ikaite research [1] included early laboratory experiments to produce ikaite that used Calgon (Na_2 ($Na_4(PO_3)_6$)) as a calcite inhibitor [28]. Following this seminal study, the role of phosphate has continued to raise interest for understanding ikaite formation. Naturally occurring ikaite in Ikka Fjord was also thought to require the natural high phosphate levels in the waters of the fjord [29], and that ikaite abundance could be controlled by porewater phosphorous concentrations [30].

In more recent laboratory experiments, it has been demonstrated that Mg^{2+} can, under the right conditions, also act as a calcite inhibitor [31]. This observation is also supported by observations from Ikka Fjord [32,33]. Laboratory experiments with conditions simulating those of Ikka Fjord are particularly puzzling as they showed that phosphate is not mandatory for the precipitation of ikaite, high concentrations in Mg^{2+} being sufficient as a calcite inhibitor, but they also showed precipitation up to temperatures of 15 °C in open beakers [32]. Even more remarkable was the experimental production of ikaite that

was stable at 35 °C [34]. Recent studies from Ikka Fjord show, however, that in natural environmental conditions, sea water temperatures above 6 °C destabilise ikaite, which alters into other calcium carbonate minerals, such as monohydrocalcite, aragonite, and calcite [33]. The authors hence predict that in a warming Arctic, the columns of Ikka Fjord will sadly change mineralogy into mainly monohydrocalcite. Such observations from natural and laboratory systems are of great interest as they can lead to a better understanding of what enables ikaite to form at higher temperatures than normal. While awaiting the geochemical breakthrough on the ikaite enigma, there is much to be gained by studying recrystallised ikaite in the form of glendonite. The term guttulatic structure, meaning little drop, was introduced [7], to describe a calcite texture found in glendonite. This term refers to the distinct zonation in mm-large calcite crystals that characterise recrystallised ikaite as previously described [35]. It has been confirmed [4,5] that in situ ikaite gathered in 1983 [16] recrystallised to calcite with a guttulatic texture. What is now recognised as guttulatic texture was also described in an initial DSDP report on the Nankai trough, where ikaite crystals were observed recrystallising to calcite on board the ship, providing the first microscopic evidence that the texture in glendonite indicates an ikaite precursor [36]. Marine sediment-formed euhedral ikaite is now unequivocally identified as the parent mineral to glendonite [4,5], in modern as well ancient marine glendonite-bearing settings [2,4,5], with guttulatic microstructure being a key identifier of recrystallised ikaite and glendonites [6,10]. This relationship has demonstrated the need to re-evaluate historical Holocene coastal sites [6], with the aim of finding a unifying geochemical agent that promotes ikaite formation zones in limited sites or horizons of vast environmental settings, such as the Wadenmeer coastline.

Identification of Glendonite

Glendonite is a monoclinic M2 class mineral with various morphologies, all consistently showing blades with pseudo-pyramidal shapes and prominent angular edges (Figure 3). Characteristics normally associated with glendonites are: crystal bending to one side, displaying a set of identical convex and concave faces with a tabular endpoint to the crystal [3]. The concave (Cv) sides comprise a repeating set of "staircases"-aligned prismatic faces, whereas the concave (Cn) side has faces which form a pseudo-pyramidal form (Figure 3). Observation of a great number of pseudomorphs with similar overall shape and petrology has resulted in confirmation of these key morphological features for glendonite identification. Poorly preserved pseudomorphs can still be identified by the diagnostic bending of the glendonite associated with a diamond shaped cross section. Using mineralogical macroscopic and microscopic observations, we can demonstrate that any glendonite will (usually) fall into one of three categories, all characterised by having a guttulatic petrology [7]. A glendonite morphology always displays a diamond-shaped cross section, while the whole crystal often shows a slight banana-shaped tilt, ending with a tabular tip (Figure 4). The three categories in Figure 4 are:

1. Category 1 (Figure 3a–c) corresponds to the best preserved glendonites bearing three key features: clear tabular tips, pseudo-pyramids on the convex side, and prismatic staircases on the concave side [3,5].
2. Category 2 will often only bear some of the common key features described in category 1, but not all (e.g., Figure 3e,h).
3. Category 3 will only show a simple morphology (one arm, single blades, . . .) and the diamond-shaped cross-cutting structure (e.g., Figure 3g,i).

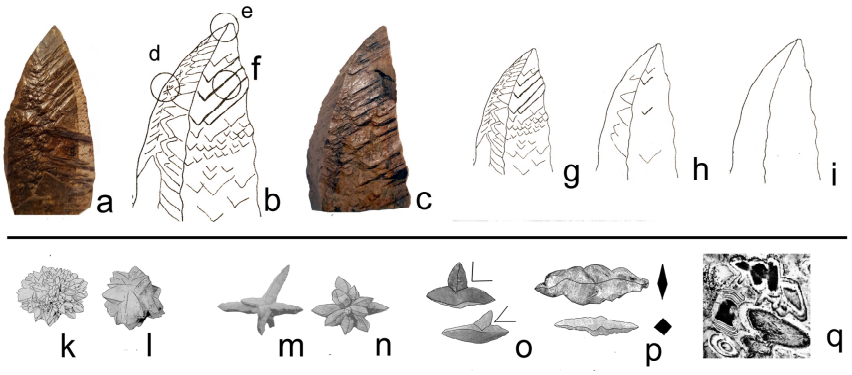


Figure 3. Glendonite is a monoclinic M2 class mineral and has morphologies that suggest twinning or penetration growth; this, and variable styles of preservation, results in considerable morphological variation. Despite this, key morphologies can be defined for recognising glendonite: a tabular tip of a four-sided body, two sets of concave and convex sides. The concave sides have arrow-shaped faces and small pseudo pyramids, the concave faces are aligned in a prismatic staircase [3]. (**a**) Fur Formation glendonite, convex side. (**b**) The morphological key points. (**c**) Fur Formation glendonite, concave side. (**d**) Convex side (Cv) "arrowheads". (**e**) Blocky tabular prismatic tip. (**f**) Concave side (Cn) "prismatic staircase". (**g**) Category 3 with all key points. (**h**) Category 2 with only some key points. (**i**) Category 1 with no distinct key points. (**k**,**l**) Glendonite morphologies [3,8], where (**k**) and (**l**) are stellar nodules defined by grouped crystal forming form one point in equal length crystals. (**m**,**n**). Clusters defined by crystals forming from one point but not grouped or in equal length. (**o**–**q**) Bladed, where (**i**) has one arm in variating angle, and Figure 3(**j**) is single blades where the silhouettes show how much a given cross-cut can vary in dimensions [3]. (**q**) The unifying petrographic texture named guttulatic [7].

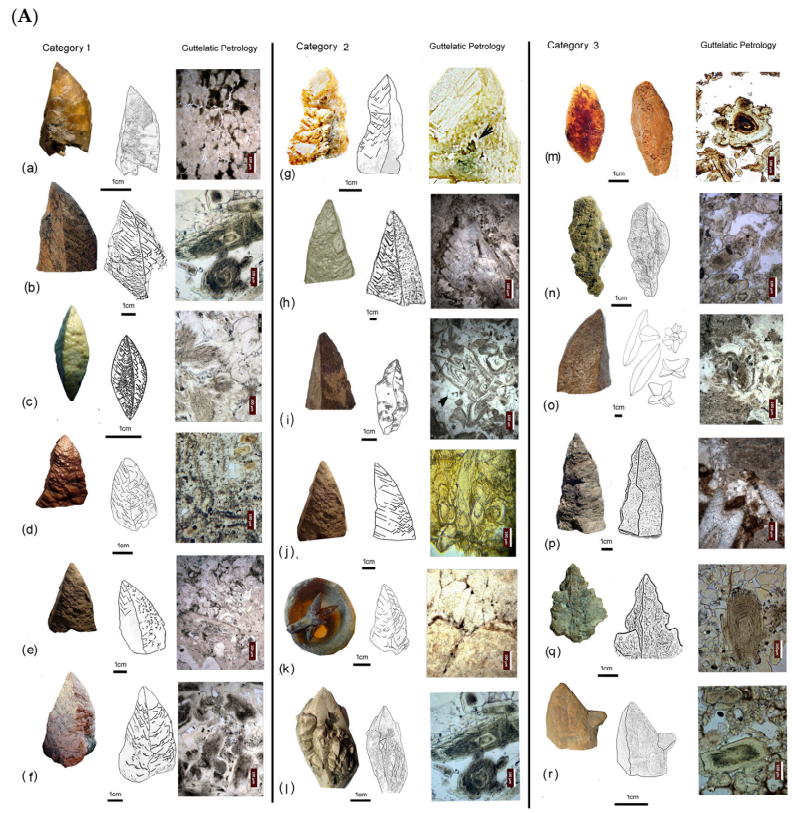


Figure 4. *Cont*.

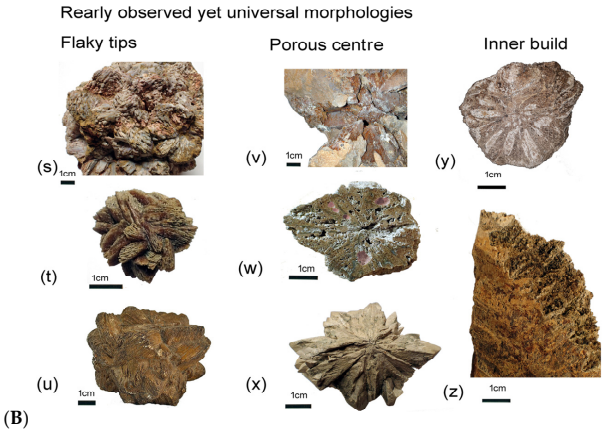


Figure 4. (**A**) A petrographic chart where samples we have physically investigated are ordered into the three categories as shown in Figure 3. All samples regardless of preservation and morphology display guttulatic texture. In category 1, nearly all morphological key points are observable; in category 2, only few; and in category 3, only the body shape and diamond-shaped cross section hint glendonite morphology. More details are provided in the Supplementary Materials, Table S1. (**B**) Morphological textures observed randomly yet consistently enough to indicate relationship to the process of ikaite recrystalising. References in Figure 4**A**: (**a**) Antarctic, South Georgia, ikaite [13,37], (**b**) Denmark, Limfjord, Early Eocene [3], (**c**) Sangerhausen [25,38,39], (**d**) Scotland, Clyde, Post-glacial [6,40], (**e**) USA, Alaska, Late Oligocene [26,41], (**f**) Russia, Olenitsa, Post-glacial [20,21], (**g**) Russia Oktomsk, Recent ikaite [18], (**h**) Australia, NSW Singleton, Permian [42], (**i**) Japan, Honshu, Late Miocene [19], (**j**) USA, WA, Late Oligocene [24,43,44], (**k**) Denmark, Silstrup, Late Oligocene [3], (**l**) Canada, Newfoundland, Late Oligocene [45], (**m**) Alaska Point Barrow, Recent ikaite [4,16], (**n**) Canada, Fundy, Post-glacial [6,23], (**o**) Australia, NSW Glendon, Permian [42,46], (**p**) Argentina, San Juan, Permian [22], (**q**) Alaska, Sarishef Island, Post-glacial [6], (**r**) Germany, Wadden Sea, Post-glacial [6]. Figure 4B(**v**,**w**,**x**), porous centres generated as ikaite stellar nodules formed, as Figure 4B(**w**) is calcite preserved as Holocene recrystalised ikaite [17] sample from site TWL2; Figure 4B(**y**,**z**), weathered inner structures that align to the outer morphology we have only observed in the mega size Danish glendonite. Figure 4**B**: (**s**) Australia, Cooper Pedy, Cretaceous [47,48], (**t**) Russia, Olenitsa, Post-glacial [20,21], (**u**) Australia, NSW Wallaby, Permian [49], (**v**) Denmark, Limfjord, Early Eocene [3], (**x**) Russia, Taymir, Cretaceous [2,50], (**y**) Denmark, Limfjord, Early Eocene [3], (**z**) Denmark, Limfjord, Early Eocene [3]. All samples are listed in Supplementary Material S1.

These three categories are likely linked to different degrees of preservation (Figure 4).

In Figure 4A, petrographic investigations show that the pseudomorphs have a guttulatic texture [7,10,35]. The morphologies have been systematically arranged into categories [8], as used in Figure 3. In Supplementary Table S1 we provide greater detail of more sites than can be included in the text.

Arctic stellar glendonite nodules were described by Kaplan [50] and Kemper [51] and from what is now known as Sverdrup basin [52]. Svalbard and arctic paleo sites are described in refs. [21,53–57]. The Svalbard sediments are spatially close, yet host glendonite from the late Jurassic [53,56], to the early Eocene [54]., with glendonite also reported from the Jurassic in Germany [58]. A similar situation has occurred in Japan, where glendonites occur in spatially close sediments with ages from the Eocene to Miocene [19]. The recent major compilations of glendonite data [2,4,5,7] reveal that glendonites (and present-day calcite after ikaite) with wide ranging morphologies and degrees of preservation are linked via guttulatic textures. By investigating such a large number of morphologies and degrees of preservation, we have identified features that potentially indicate a connection to the way ikaite recrystalises. The flaky tips of glendonite are possibly being generated epimorphic from cleavage in ikaite, preserved during recrystallisation Figure 4B(s,t,u).

5. Spectacular Morphologies from Historic Sites United by Guttulatic Petrography

Reviews [1,2,59,60] of historical records reveal that key glendonite characteristics were already apparent in the earliest descriptions and illustrations, e.g., [38]. Both Dana's account of Mono Lake [38] and the more recent investigation [7] document the presence of guttulatic textures, consistent with observations from multiple historic sites [6]. The utility of guttulatic textures for glendonite identification is highlighted in a review of the Olympic Peninsula site (Figure 5a–h). This site, first described in detail by Dana [38], has been meticulously analysed in terms of geochemistry and stratigraphy.

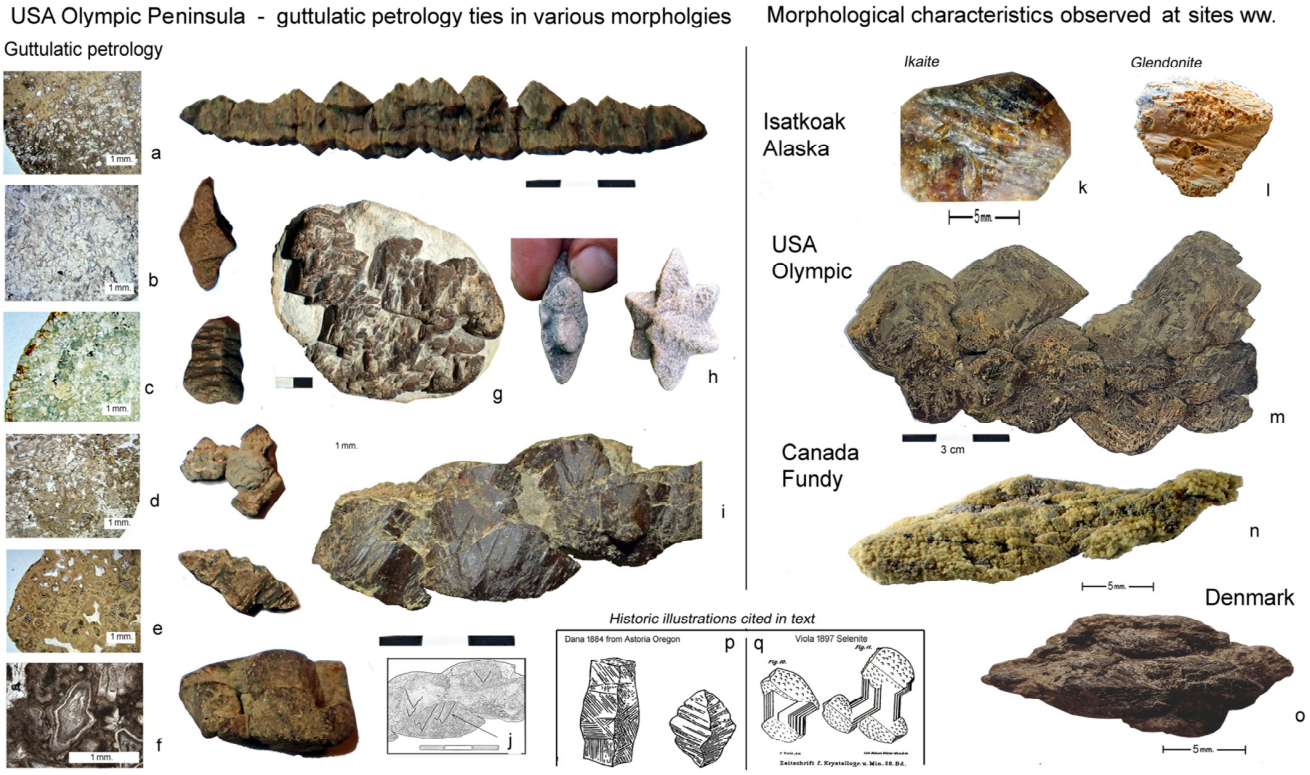


Figure 5. Widely differing glendonite morphologies. (**a**–**i**) are from Olympic Peninsula, (**a**,**d**,**i**) Washington State, USA, Deep Creek (finder Leo Scarpelli), (**b**,**c**,**e**,**f**), Mudrock Beach. (**a**–**f**) shows guttulatic petrology, supporting the statement that all presented shapes formed as ikaite. (**i**,**j**) from Deep Creek is the only example with arrowhead faces on the concave side. (**g**) multiple repetitions much resembling structure observed from selenite twins. Some of the samples barely resemble typical glendonite morphology, their identity only confirmed from their guttulatic petrology. (**h**) is a double penetration growth (photo John Cornish). (**k**–**o**) illustrate the structure of parallel repetition from Olympic peninsula can be observed in three very different settings, whereby suggesting the observation relates to the mineral. (**k**) glendonite from Point Barrow in Alaska, (**l**) recent ikaite from Point Barrow in Alaska. (**m**) late Oligocene Mudrock Beach, Washington State. (**n**) is from Bay of Fundy. (**o**) late Oligocene Silstrup, Denmark (finder Inge Marie Dahlgaard Krog). (**p**) Edward Dana's 1884 sketch of Astoria samples [38]. (**q**) the parallel selenite growth illustrated in ref. [61], which demonstrates how monoclinic M2 mineral selenite can exhibit parallel repetition along 010 cleave plain. Ikaite is of the same symmetry class, which suggested a shared genetic link.

Other significant glendonite-bearing sites include the North Alaskan Nuwok Member margin, the north-western Pacific margin [24,43], and the Sagavanirktok Formation—a vast unit extending from northern Alaska along the Pacific coastline to northern California. Additional sites include Carter Creek, Alaska, USA [26,41], and further south along the Cascadia NW Pacific margin [43,44], where both morphologies and petrology have been

examined. The Olympic Peninsula site stands out due to its high morphological diversity, particularly a feature of parallel crystal repetition, which warrants further investigation (Figure 5k–o).

Collectors such as Leo Scarpelli and John Cornish from Seattle, Washington, have contributed unique samples from the Olympic Peninsula (Figure 5), enriching our understanding of glendonite morphological variation. Penetration growth angles versus cluster formation have been discussed previously [3], with Figure 5h being a prime example of penetration growth in a single plane. While penetration growth had previously been hypothesised, it was not confirmed as a distinct morphological feature until now. This suggests that clusters without hollow centres form through penetration growth, whereas stellar glendonites with crystal arms radiating in multiple directions often display a central void, which is not observed systematically, and therefore not included in Supplementary Table S1. Also, occasionally, flaky tips occur, where the external structure does not reflect the inner morphology only on the surface.

Another remarkable growth form is the elongated, single-bodied glendonite featuring a series of "arrowhead" structures on its convex side (Figure 5i,j), Parallel crystal repetition is well documented in selenite [61] and occurs along the 010 cleavage plane referred to by finder Leo Scarpelli as "pyramidite structur" (Figure 5a), where the "arrowheads" of the convex side form a parallel repetition, yet its only at this site that such detail has been observed. As selenite and ikaite belong to the same symmetry class and space group in (monoclinic m2), this suggests a potential genetic link. The possible symmetry axis and cleaves will be addressed in the next paragraph.

The parallel repetition structure has also been observed in ikaite from Barrow (Figure 5k) and the Kara Sea in sample T169 (not shown, pers. Comm, Alexey A. Krylov), as well as in glendonites from three different sites, being Silstrup (Denmark), the Bay of Fundy, and the Olympic Peninsula (Figure 5k–o), suggesting that this behaviour is related to ikaite and can be seen preserved in glendonite after recrystallisation.

5.1. Preliminary Observations of Ikaite Cleavage Suggest Symmetry Alignment

The study of glendonite crystallographic symmetry has a long history, beginning in 1826/27 [1,2], where it was described. Since crystallographers such as Victor Goldschmidt in 1913 [62], and 1923 [63], Carl Hintze in 1915 [64], and earlier Gerhard Blum in 1867 [65] all studied the mysterious glendonites, leaving this mineral as one of many unsolved geological enigmas. In 1913, Victor Goldschmidt published a series of books known as "Atlas der Krystallformen" [62], which includes thousands of neat crystal symmetry drawings of pseudomorphs [63], Band 9, Tafel 118 to 125, Figs. 30 to 147 on calcite, and Band 4, Tafel 63 to 73, Figs. 1 to 179. Ref. [63] described these minerals as forms of selenite; however, we observe no clear crystallographic depictions that hint at any relation to the many morphological observations that we have made on ikaite and glendonite. Selenite is, however, of interest, as it forms in sediments and it is of the same monoclinic M2 symmetry class as ikaite. In the years up to 1913, ikaite was only known from laboratories, and the origin of glendonite was unknown [1,2,60].

However, it was not until 1982 that euhedral ikaite was documented [27]. Only a few studies have attempted to analyse ikaite crystallography, notably [66] on ikaite from Shiowakka Springs and, more significantly [9], which demonstrated, via neutrino spin analysis, that ikaite's lattice, observed in both laboratory settings and Ikka Fjord, can accommodate flexible distortions—potentially induced by organic interactions. This flexibility may account for the formation of euhedral ikaite in marine sediments [13]. This finding is particularly relevant to our study of an ikaite crystal from the Annekov Trough on the southern shelf of South Georgia, retrieved from 359 m of water depth and 570 cm of

sediment depth (GC-16, GeoB 22049-3 in ref. [14]. This sample was later examined by Vickers et al. [15] to track the transformation from ikaite to glendonite. A key novel observation is the presence of cleavage in the ikaite crystal—an unprecedented discovery due to the mineral's extreme metastability. The suspected cleavage is illustrated in Figure 6a,b, showing the crystal splitting while stored at −18 °C at MARUM. The cleaved ends are depicted in Figure 6c,d, with the larger half investigated by Vickers et al. [10] and the smaller by Schultz et al. [5]. While conducting scanning electron microscopy (SEM) at Lund University, Carl Alwmark captured the cleavage pattern, revealing a surface comparable to a true cleavage plane (Figure 6f1,f2), as the only known photograph of ikaite where straight-lined cracks might indicate cleavage. However, due to the crystal's disintegration [15], further investigation of true cleavage beyond the images was not possible.

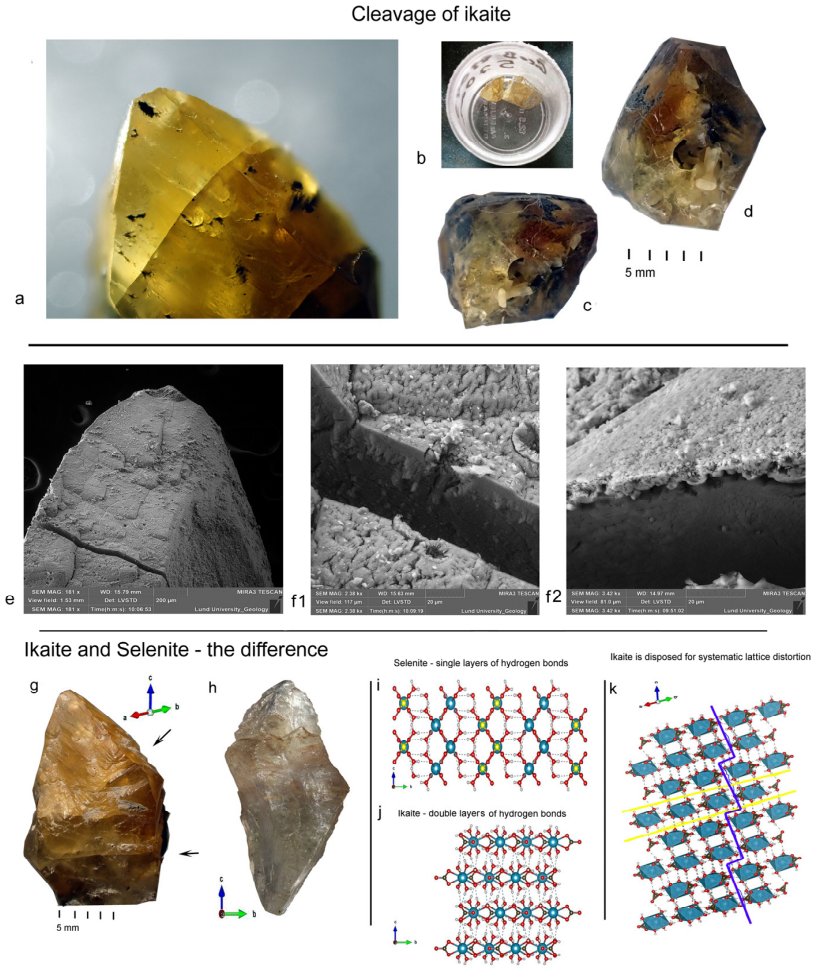


Figure 6. Ikaite crystal GC-16, GeoB 22049-3 from South Georgia showing cleavage and growth (**a**). (**b**) ikaite crystal GC-16, GeoB 22049-3 having split in MARUM's cold storage (photo Gerhard Bohrmann). (**c**,**d**) the true ikaite cleavage and internal signs of recrystallising. (**e**) smallest end of (**c**) monitored in SEM: the ikaite crystal splitting again, with the same (estimated) cleavage angle a few minutes into the early stages of full recrystallisation (photo by Carl Alwmark). See ref. [10] for details. (**f1**) the cleavage of ikaite enlarged, (**f2**) the surface is porous type 0 calcite forming on ikaite, with whitish dots of calcite presumed to be type 1 forming. (**g**) the ikaite crystal with suggested axis distribution, and cleavages indicated by arrows. (**h**) ikaite with corresponding hydrogen bonding layer is present. Ikaite exhibits two weak hydrogen bonding layers perpendicular to the c-axis (**i**) yellow lines. A possible secondary cleavage plane is marked in blue. (**h**) a lenticular gypsum (selenite) crystal for comparison. (**i**) the crystal structure of gypsum is, like ikaite, defined by weak hydrogen dotted bonds in (**j**), forming layers perpendicular to the b-axis, which aligns with the (010) cleavage plane. (**k**) shows the difference created by double hydrogen bonds of a distortable lattice.

Both gypsum and ikaite share the monoclinic m/2 system and the same space group C2/c. This makes gypsum an ideal structural analogue for interpreting the few available ikaite cleavage images. The crystal structure of gypsum is defined by weak hydrogen bonds (dotted bonds in Figure 6i), forming layers perpendicular to the b-axis, which aligns with the (010) cleavage plane augmented by parallel repetition and shown in (Figure 5k–o). Similarly, in ikaite (Figure 6h), a corresponding hydrogen bonding layer is present but perpendicular to the c-axis, indicating a (001) cleavage—consistent with the cleavage observed in our ikaite sample.

Interestingly, ikaite exhibits two weak hydrogen bonding layers perpendicular to the c-axis (Figure 6i yellow lines). Additionally, we have identified a possible secondary cleavage plane (marked in blue, also in Figure 6i), which does not extend uniformly through the structure but rather shifts between calcium polyhedra in a staggered pattern. This discontinuity may explain the stepped surfaces observed in ikaite and the concave morphologies of glendonite.

As a monoclinic m/2 mineral with centrosymmetry, ikaite is susceptible to polysynthetic twinning (such as repeated or albite twinning) along the c-axis (001). A novel hypothesis is that euhedral ikaite in marine sediments forms via pseudo-merohedry, as described by the Law of Mallard [67]. This law states that twinning involves the loss of full symmetry, with certain lattice elements no longer perfectly mirrored. This could explain two key differences between lenticular gypsum and ikaite:

1. Gypsum's prismatic faces exhibit perfect mirroring, whereas glendonite prismatic faces do not [3].
2. Gypsum typically has pointed terminations, whereas glendonite has tabular prismatic tips.

This suggests that structural distortions during ikaite crystallisation influence the final morphology of glendonite, as suggested by ref. [9].

5.2. Frequently Shared Petrographic Structures

The petrography of glendonite shown in Figures 4 and 5 has been extensively documented in [4,7,10,18,34,58]. Ref. [35] described the petrography of glendonite from the Black Alley Shale (Permian, Australia) and the Fur Formation (Early Eocene, Denmark), identifying three calcite generations:

1. Type 1: Zoned primary calcite grains
2. Type 2: Spherulitic calcite
3. Type 3: Later infill spar

Our current research expands on refs. [7,8,35] by showing that Type 1 calcite in the Fur Formation exhibits two distinct subtypes:

1. Guttulatic texture (Greek for "little drop"), characterised by a zoned internal structure.
2. Non-zoned texture, lacking apparent internal differentiation.

These subtypes also differ in their Mg content, as illustrated in Supplementary Petrographic Charts S1 and S2. The role of Mg in ikaite formation has been highlighted by refs. [31,32], while the Backscattered Electron Imaging (BSEI) and Energy Dispersive Spectroscopy (EDS) data in Supplementary Petrographic Chart S2 also suggests that Mg influences the microstructure of primary calcite in glendonite. Importantly, this differentiation is not exclusive to the Fur Formation; similar patterns have been identified in Olenitsa (Russia) and other sites.

High Mg concentrations have also been observed in samples from the Sea of Okhotsk [6,18]. To further investigate and classify these petrographic features, we build upon ref. [8], who systematically classified glendonites based on morphology and optical

characteristics in Frank's work, expanded to incorporate guttulatic textures. This structure has been observed at numerous historical glendonite sites, including Nankai Trough, where zoned primary calcite grains are thought to represent recrystallised ikaite [35,68].

The transformation of ikaite into calcite and its internal cementation in glendonite have been well documented [10]. Refs. [4,5] analysed the morphological and petrographic changes occurring during ikaite recrystallisation in cold-stored samples from the Laptev Sea and Isatkoak Lagoon (Barrow). Comparisons with older samples from Nankai (collected 2012) and South Georgia (collected 2016) suggest that, even when preserved in cold storage at Bremerhaven and GEOMAR, ikaite undergoes partial dehydration over time. Similarly, Stockmann et al. [32,33] observed natural ikaite dehydration in the older sections of Ikka Fjord tufa pillars.

A recent study from Expedition 396 to the Norwegian Trench [11] reported Late Paleocene/Early Eocene glendonite containing Type 0 calcite, which forms early in the ikaite-to-calcite transformation. This may explain why all glendonites lack sediment infill despite the ikaite-to-calcite transition theoretically producing a pseudomorph with 31% mass loss and 69% void space.

Stable isotope analyses have demonstrated that ikaite precipitation occurs at the boundary between the microbial sulphate reduction zone and the methanogenesis zone [13]. Burial rates also play a crucial role in glendonite petrography and isotopic composition [2,15]. In the Danish Fur Formation, there is no systematic distribution of concretion-encapsulated versus non-encapsulated glendonite within the same horizon. However, in New South Wales [8,42,49] and the Arctic Sverdrup Basin [52], most glendonites are not encapsulated.

Examination of the primary calcite grains (i.e., the calcite that first replaces ikaite) in glendonites from Australia, Japan, and Denmark [35] has shown that they have universal petrographic characteristics. The distinct zonation of the calcite, that in daylight appears whitish, appear black in plane polarised microscope light, due to its sweeping extinction [8]. In certain orientations, the calcite grains tend to display colour undulation intensity, due to the birefringence of calcite. Another feature common to all glendonites is that they are free of sediment infill, despite the fact that the recrystallisation process creates a hollow pseudomorph that is practically (at 51.4%) uncemented [6,68]. Refs. [16,68] speculated that the volumes of water and calcite exceed the original volume of ikaite, whereby the porous pseudomorph would expel water released from the ikaite. Alternatively, the space in the pseudomorph may be protected from the sediment by a rim of calcite formed around the ikaite crystal margin [3,5,11].

Our findings add two novel petrographic observations:

1. Sweeping extinction in Type 1 calcite grains is possibly caused by weak chelate bonding of organic ions to calcite surfaces [69].
2. Dendritic ("fir-tree") zoning, likely resulting from sector zoning and fluctuating Mg concentrations [70].

Further research into Mg incorporation during ikaite recrystallisation may clarify these patterns, contributing to a more comprehensive understanding of glendonite formation. Images of sweeping extinction and dendritic zoning from a number of well-documented sites are included in the Supplementary Materials Charts S1 and S2.

5.3. Glendonites from the Limfjord of Denmark

Two sites in Limfjord region are known to have glendonites [3]: one is Silstrup of the late Oligocene age, equivalent to the Olympic Peninsula and Alaskan Carter Creek both in the USA, the other is the Fur Formation of early Eocene age contemporaneous with glendonite from Paleocene/Eocene sites on Svalbard [54] and the Norwegian Trench [11].

The Fur Formation, type profile at Knude Klint on Fur Island [71], shown in Figure 7 was deposited directly above the older Ølst Formation [1,15,71], where dark clay layers include the PETM interval [72–77]. The regional correlation of the PETM and the North Atlantic Igneous province (NAIP) has also been demonstrated using Tellurium concentration in sediments [78]. In addition to hosting mega-size glendonites, the Fur Formation is significant for palaeobiological research due to its exceptional preservation of biogenic soft tissues [79–84]. The remarkably diverse palaeo flora and fauna of the Fur Formation, including many first occurences of modern flora and fauna is discussed in Simonsen [85] and Schroeder [86]. A full geochemical analysis of Fur Formation glendonites [87] is available open source via Münster University's Miami server.

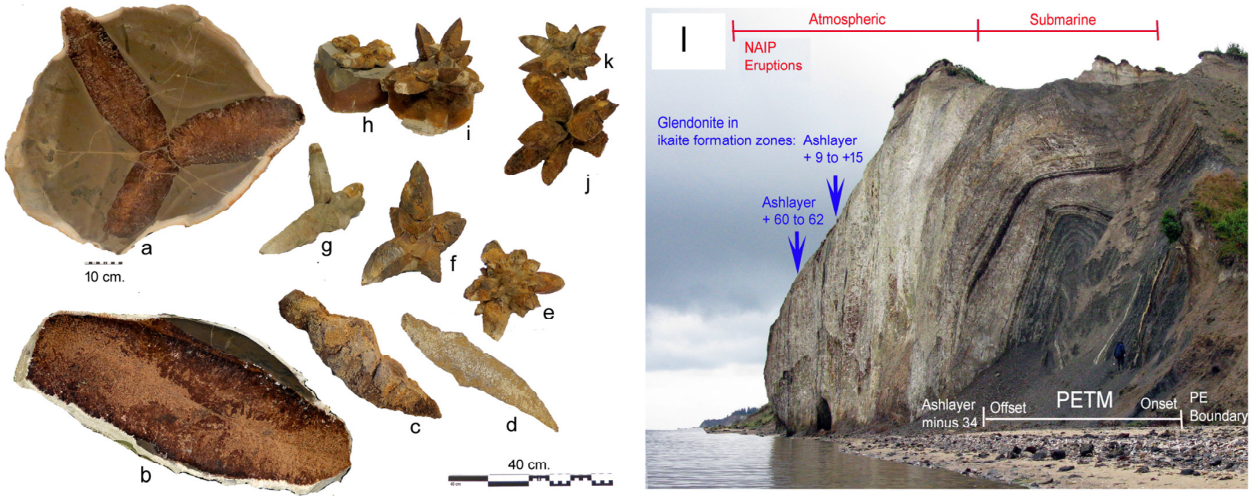


Figure 7. Fur Formation glendonite: (**a**–**i**) Various mega-size glendonites (**a**,**g**,**h**,**e**,**i**) from the Fur Formation retrieved from shown site Knude Klint. (**b**,**h**) is from Ejerlev (photo Henrik Madsen), (**c**) (collected by Hans Christian Christensen) & (**d**,**g**,**i**,**k**) (collected by Palle Christensen) from Hestehave quarry, both on Fur Island. (**f**) is Danekræ number 56 from Skarrhage quarry, all from the Island of Mors. Glendonite from Kundeklint (**a**,**i**,**j**,**k**) (**l**) Knudeklint site showing the early Eocene Fur Formation is a marine diatomite with over 180 interbedded volcanic ash beds; it includes two levels that would appear to be paleo IFZs, now outcropping as mega size glendonite [1,3,15]. The black ash layers are mostly tholeiite basalt. The pale ones are rhyolitic [88].

As shown in the accompanying Figure, possible calcite inhibitors vary even within the Fur Formation, a phenomenon that remains unexplained, as does the presence of ikaite formation zones occurring just 300,000 years after the PETM thermal maximum. These unresolved questions warrant further investigation, an endeavour facilitated by the excellent preservation of glendonites in the Limfjord coastal cliffs and the site's accessibility. Additional advantages include the well-constrained stratigraphy [1,3,71,88–91].

Data from the Fur Formation remain inconclusive regarding whether Mg^{2+}, PO_4^{3-}, organic material, or volcanic nutrients are the key factors enabling ikaite formation. Carbonate diagenesis in the Fur Formation occurred at pH values ranging from 5.5 to 8 [79,82,92]. Bottom water temperatures have been estimated at >5 °C based on Δ47 analyses [15], while diagenetic temperatures did not exceed 38 °C [84,93]. Estimated water depths ranged from 200 to 400 m (equivalent to 200–400 kPa), based on ichnofacies evidence, including bathyal Zoophycos in the late Palaeocene Holmehus Clay and sublittoral Teichichnus in younger early Eocene Fur Formation sediments [71,91]. This transition from bathyal to sublittoral depths suggests shallowing, likely due to uplift from the North Atlantic Igneous Province.

At the onset of Fur Formation deposition, the basin was highly restricted. Evidence from the North Sea and Norwegian margin suggests this isolation occurred between ~56 and 54.6 Ma. The subsequent opening of the Faroe-Shetland Basin restored access to global

oceans, but much of the Fur Formation was deposited under restricted conditions [76]. Sea surface temperature (SST) reconstructions using TEX86 [73] indicate a 10 °C increase during the PETM onset, reaching up to ~33 °C, followed by a gradual decline to post-PETM values of 11–23 °C. Notably, the PETM saw a global temperature increase of ~6–8 °C over ~5000 years, driven by large-scale greenhouse gas emissions [77]. Local paleoenvironmental and glendonite precipitation conditions following cooling are detailed in [1,15].

The Fur Formation glendonites are among the best-preserved globally [3]. The largest known mega-glendonite cluster, measuring 1.6 metres in width with 16 arms, has an estimated volume of 41,500 cm^3, equivalent to a 75 kg ikaite cluster (density of ikaite = 1.78 g/cm^3). These glendonites are often encased in calcite concretions, the largest of which measure ~8 m wide and contain ~20 tons of calcite. The Fur Formation has seventeen horizons with nodular or bedded calcite cement, and three silicified shale beds with large calcite concretions [71,92]. In these settings, only two have glendonite indicating paleo ikaite formation zones.

In the Danish Limfjord region, two IFZs occur 29 million years apart [3]. In Japan, IFZs are recorded from the Late Eocene, Oligocene, Miocene, and present-day Nankai Trench [1,5,36]. The combination of detailed stratigraphy, well-documented paleoclimate records, and exceptional fossil preservation enables a robust understanding of the paleoenvironmental conditions that favoured ikaite formation and its potential role in the carbon cycle. Notably, glendonite preservation is concentrated within specific stratigraphic horizons [3,13]. Precipitation of ikaite may have been relatively rapid [1,29,33].

6. Potential for Carbon Capture and Storage

The massive size of Danish mega-glendonites and their enclosing calcite concretions suggests significant carbon fixation, raising interest in their potential role in natural carbon sequestration. The Fur Formation has seventeen horizons with concretions [71], of which only two are IFZs with glendonite [1,3] that occurs both with and without enclosing concretions, as shown in Figure 7. This is commonly observed worldwide, as some sites have large numbers of unenclosed glendonite, whereas other sites have glendonite encased in calcite concretions (Supplementary Table S1), a key observation being that the glendonite always predates the concretions. Ikaite may facilitate the precipitation of stable calcite from atmospheric CO_2, a process relevant to carbon capture strategies [15,94,95].

However, for this to be viable, the mechanisms enabling ikaite formation at normal pressure and low temperatures in non-extreme environments must be better understood, as we hope to display in Figure 8, that discloses the broad span of environment in which ikaite forms—extremes as non-extreme.

Of special interest is the data in Stockmann et al. [94], as it presents the fundamental interaction between microbiology and geochemistry occurring in Ikka Fjord, where co-author Erik Trampe has achieved early-stage success in his Ikkaton project, turning CO_2 into $CaCO_3$ via ikaite synthesis. For instance, ikaite has also been observed forming in frozen shrimp [96,97] and bacterial smears on the surface of washed-rind cheese [98], and in bacterial slime flux jelly in tree wounds in the Sonoran Desert during winter cold snaps [99]. Laboratory studies have synthesised ikaite at higher temperatures than those recorded for natural occurrences. Milodowski et al. [100] precipitated ikaite at elevated pressures and temperatures between −3 °C and 14.3 °C, while Tollefsen et al. [34] managed to form ikaite at atmospheric pressure at 35 °C and pH 9.3–10.3 using a seawater-sodium carbonate solution. Ref. [101] produced ikaite in a refrigerator, though their solution was artificial and the resulting precipitate lacked typical ikaite morphology. Understanding discrepancies between natural ikaite formation (often at <8 °C and pH < 8) and laboratory conditions could provide insights into its role in carbon capture and storage.

The presence of Mg^{2+} [31,32] and PO_4^{3-} [30] has been shown to inhibit calcite precipitation and favour ikaite formation. Holocene ikaite occurrences span a pH range of 7–11, but no clear link has been established between ikaite formation and specific pore fluid geochemistry shifts. This suggests a potential biogenic influence, possibly involving bacterial activity or enzymatic processes, with volcanic ash providing nutrients that enhance biogenic activity [95].

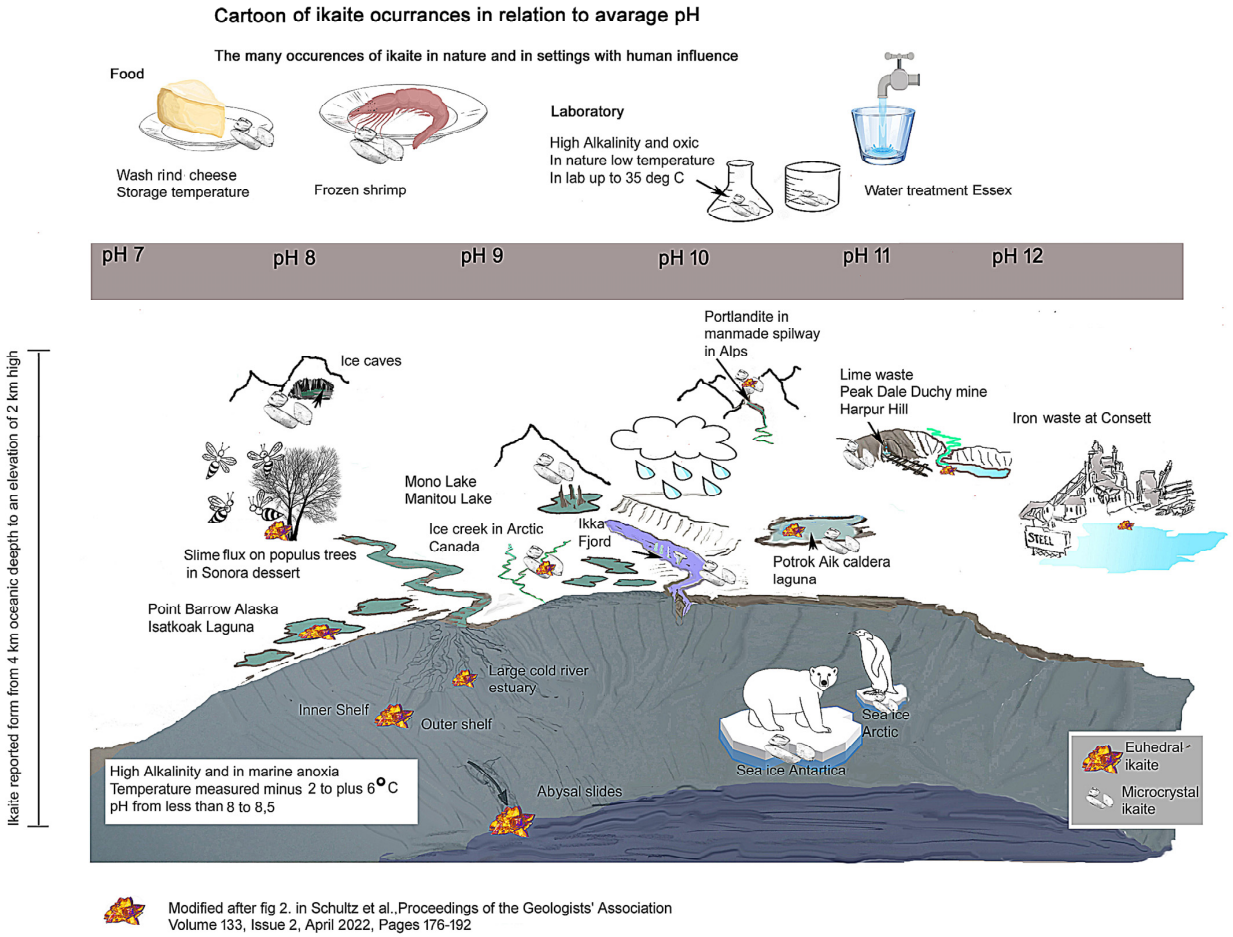


Figure 8. The broad range of settings spaning from the deepest abysal slides to marien shelf, with natural precipitation of ikaite in modern sediments, along a fine variety of human influenced settings. Microcrystalline ikaite apparently rapidly builds up large masses in Ikka Fjord [27], whereas large euhedral ikaite crystals form in marine shelf sediment, e.g., [1]. Examples of Abyssal [17,36,102], Outer shelf [12,14,103], Inner shelf [18,104,105], Estuary [12,104,106,107], Sea Ice [108,109], Ikka Fjord [29,110]. Examples of natural ikaite from terrestrial setting: Isatkoak lagoon [4,16], Mono Lake [111], Manitou prarie lake [112], Canada saline spring [113], Japan Shiowakka spring [66], Potrok Aik caldera [114], Ice Caves [115], Slime Flux [99] and in food; Frozen shrimp [96,97], Cheese [98]. From laboratory we can give examples like [28,101,116–119], and human influended settings in nature like: Essex waterworks [120], Alps water akavduct [121], Peak dale tunnel [122] Harpur Hill line waste [100] Consett inron waste [123].

We have not been able to produce a complete data set (Table 1) for Figure 8, but this is included in the Supplementary Materials, Table S2 regarding Holocene ikaite formation showing the specific conditions vary, with Mg^{2+} being of particular importance, which is consistent with the observation that Mg concentration varies consistently with the calcite types generated when ikaite recrystallises (e.g., calcite cement in Fur Formation glendonite, listed in Supplementary Materials Chart S2).

Table 1. Four selected sites out of 28 entries in Supplementary Materials Table S2. All the given references have data, but only for these four were pH, salinity, temperature PO_4^{3-}, Mg^{2+}, and SO_4^{2-} data are available. The below plot (Figure 9) complements Figure 8 showing sites and settings, with all available date in Supplementary Materials Table S2.

	pH	Temperature	Salinity	PO_4^{3-}	Mg^{2+}	SO_4^{2-}
		°C	g/L	mg/L	mg/L	mg/L
Bransfield [13]	7.7	−1.5	34.5	14.4	127	5
Shiowakka [66]	6.7	<1	0.1	0.18	190	15.6
Sonora Desert [99]	8.2	<5	0.8	0.21	11.12	51.8
Ikka [29,32]	10.2	3.5	31	23	65.9	345

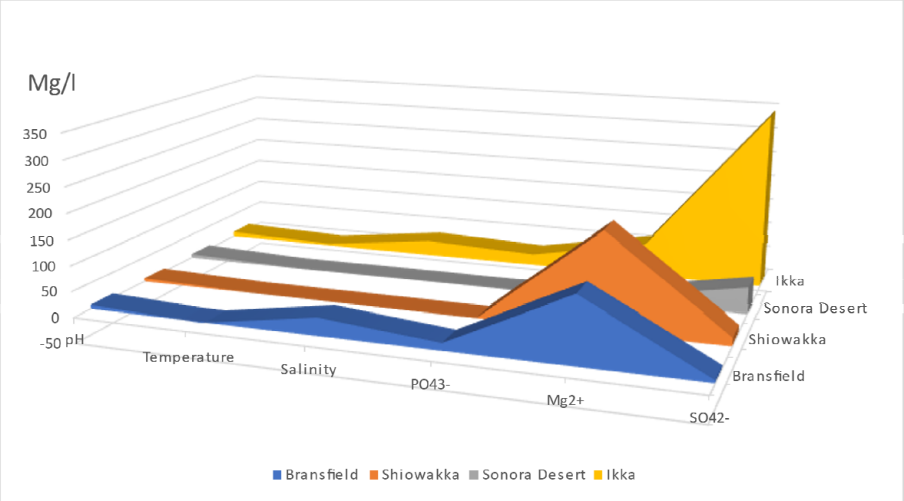


Figure 9. Complements Figure 8 by illustrating site characteristics and settings.

7. Conclusions

Geologists have long debated the relationship between the metastable mineral ikaite ($CaCO_3 \times 6H_2O$), found in modern cool-water environments, and its calcitic pseudomorph, glendonite, which appears throughout the Phanerozoic sedimentary record (e.g., [2]). Submerged ikaite tufa pillars in Ikka Fjord bear little resemblance to glendonites [29]. However, large yellow/orange euhedral ikaite crystals with typical glendonite morphology have been documented in the Bransfield Strait, offshore Antarctica [13,14,107] and in eustuaria from sibirian rivers [12,104,106].

A complete examination of ikaite morphology has been hampered by the fact that the metastable mineral decomposes above ~7 °C into wet calcite granules within hours, hindering traditional crystallographic studies. These mm-sized calcite granules form a distinctive guttulatic microstructure, observed in many marine and terrestrial settings [4,7], which, combined with morphological key points [5], can assist in determining if a given object preserved as calcite, could be related to glendonite, with ikaite as a precursor mineral. We have in this article applied the criteria evolved in this study to museum collections. Where morphology is not well-preserved, petrology can be unambiguously used, thereby extending the glendonite classification of [8] and ultimately, via petrology, adding more confirmed sites to the many previously published sites [1,2]. Following the law of Mallard [67], and using measured cleavage axes, it may be possible to include the frequent calcite twining in recrystallised ikaite as identified by Nemeth [124]. Our observations of ikaite morphology and observed ikaite cleavage provide the basis for the gifted crystallographer to model from. Naturally formed ikaite has so far only been observed as a cold-water mineral, and

stable isotope data appear to confirm this. IFZs are therefore concluded to be cold water/sediment deposits that predate other carbonate diagenetic phases. However, the reason for experimental ikaite being precipitated at higher temperatures [34] remains enigmatic. Ultimately, a deeper understanding of the biological and geochemical catalysts promoting ikaite formation could unlock new possibilities for carbon sequestration. However, the precise mechanisms remain unresolved, highlighting the need for further research. As can be seen from ref. [2], some time periods have significantly more glendonite occurrences, from which we continue to obtain sample material to examine as meticulously as in this article. One such interval is the late Oligocene [3,19,24,26,125], another is Svalbard, where glendonite observed in situ in sediment ranging from late Jurassic to early Eocene [53–57].

Supplementary Materials: The following supporting information can be downloaded at: https://www.mdpi.com/article/10.3390/min15040410/s1, Supplementary Material S1 comprises data for the Museum Salling's collection of glendonite and recrystalised Holocene ikaite, catalogued with details. Collection information on biota and sediments from Early Eocene Fur and Oelst Formations can also be found in SPECIFY, along with catalogued glendonite. Petrographic Chart S1 illustrates the guttulatic morphology [7], plus specific observations of sweeping extinction and dendritic growth noted by Frank in 2008 [8] and also shown in the samples we examined, Chart S2 illustrates how in the Fur Formation Mg is incorporated mostly in type 1 calcite, (based on 670 point analyses). Chart S2 illustrates the petrography of the Fur Formation glendonite [3,15,35]. Tables S1 and S2 elaborate data shown in [1,3]. Table S1: Denmark, Limfjord [3], Arctic, Russia, Laptev Sea [5,106], Alaska, Sarishef Island [6], Germany, Wadden Sea [6], Netherlands Vattenmeer, [6,126], Scotland, Clyde [6,127], Bransfield [13], Antarctic, South Georgia [14], Alaska Point Barrow [16], Japan, Nankai Trough [17], Russia Oktomsk [18], Japan Honshu [19], Russia, Olenitsa [20,21], Argentina San Juan [22], Canada, Fundy [23], USA, WA [24,43,44], USA, Alaska [26,41], Germany Sangerhausen [25,38,39], Argentina, Australia, NSW Singleton [42], Russia, Taymir [2,50], Canada, Ellesmere [52], Australia, NSW Glendon [46], Canada, Newfoundland [45], Germany, Wolfsburg [58], Australia, NSW Wallaby [49], Australia, Tasmania [49], Russia [21,50], Australia, Cooper Pedy [47,48], Svalbard [56,57], Scotland, Jarrow [68]. All sites from which data in this article evaluates some 1200 examined samples from primary Fur Museum and Fossil Moclay Museum on the Mors research collection, along BMNH, SNM, HMM. Table S2 contains the data that underlie Figures 8 and 9. Laptev Sea [12,106], Bransfield [13,27], Anakov Trough [14], Point Barrow [15], Keendy Isatkoak [16], Nankai Trough [17], Sea of Okthosk [18], Ikka Fjord marine tuff towers [27], Brooks [28], Argentine Basin [30], Anakov Trough [37], Shiowakka [66], Congo deep sea fan [102], Disco Bay [103], Kara Sea [104], Saanich inlet [105], Penninsula at, Firth of Tay [107], Sea ice Rysgaard [108], Sea ice Dieckmann [109], Pauli [110],Mono Lake [111], Manitou [112], Ellesmere, Expedition Fjord [113], Patagonia at Potrok Aik [114],Nemeth Victoria Cave, South Ural [115], Sonora Desert [99],Shrimp [96,97], Tansmann [98],Shaikh [101], Marland [116], Hu [117], Lazar [118], Tollufsen [119], Slack Essex [120],Graz [121], Fields Peak Dale [122], Harpur [100], Consett [123].

Author Contributions: Conceptualization, B.P.S. and J.H.; methodology, J.H.; software, B.P.S.; validation, B.P.S. and J.H.; formal analysis, B.P.S.; investigation, B.P.S.; resources, B.P.S.; data curation, B.P.S.; writing—original draft preparation, B.P.S.; writing—review and editing, J.H.; visualization, B.P.S.; supervision, J.H.; project administration, B.P.S.; funding acquisition, Museum Salling. All authors have read and agreed to the published version of the manuscript.

Funding: This research was funded by Museum Salling.

Data Availability Statement: Museum Salling—Fur Museum and Museum Mors—Fossil and Mo Clay Museum by the Limfjord are state authorized museums, under the Danish Ministry of Culture operating under the guidelines of ICOM, wherefor all data and samples are open for research by peers.

Acknowledgments: We are indebted to the late Douglas Shearman, Alec Smith, and Erwin Suess, who initiated and encouraged our interest in ikaite and glendonite. We thank MDPI editors for assistance and reviewers for vastly improving this article. Profound thanks also to colleagues Nicolas Thibault, Bas V.d. Schootbrugge, Clemens Ullmann, Morgan Jones, Johan Lindgren, Peter Németh, Henrik Friis for helping to improve this article. We thank Gerhard Bohrmann of MARUM for letting us work on ikaite crystal (GC-16, GeoB 22049-3) from South Georgia, to Jens Greinert for offering us the samples from site TWL 16-1/2 presented in [18], to Alexey A. Krylov for use of the image of ikaite stellar nodule from Laptev Sea. Thanks for Alaska samples to George L. Kennedy and Robert Spielhagen for the Svalbard samples. To Museum Salling (Fur Museum) and Fossil Moclay Museum on Mors, holding large collections from Fur Formation (Mo Clay) and Oelst fm. (PETM), we can only express the greatest gratitude to the many peers that visit. Special thanks to young PhD and Post-Doctoral workers Ane Elise Schrøder [86] (University of Copenhagen), Thomas Simonsen [85] (Museum of Natural History in Aarhus), and Nils Baumann [78] (University of Nordbayern), whose palaeontological and PETM research has informed our understanding of Fur formation. Here too, we can add that our collections, among the listed 680 samples in supplementary, are available for further research. As stated, this article summarises some 30 odd years of gathering information, so the list of peers is long, as acknowledged in [1,3–6,35]. Here special thanks to Madeleine L. Vickers for much support, and to late Erwin Suess for the encouragement to amass all my observations and present them for others to gain from. Observations accumulated from the listed museums, among them, the German marine research institutions GEOMAR and MARUM. Without support and samples from mentioned, collectors from many continents have contributed to Fur Museum's vast collection of glendonite in this article. Special thanks to the talented amateur geologist Leo Scarpelli and John Cornish of USA, along with Inge Marie Dahlgaard Krog, DK, and lastly for Bay of Fundy material Dana Morong, US, Donald Hattie, Canada. We thank Carl Alwmark form University in Lund for capturing the image of ikaite cleaving during recrystallization. Finally, a very special thanks from Bo Schultz to co-author Jennifer Huggett, to whom I was introduced in 1994 by Douglas Shearman (1918–2003), with the kind advice that one day new insight would reveal keys to solving the enigma of ikaite and glendonite. The first author being quite dyslectic, it would never have been possible to complete our sequence of six articles without the unwavering support of my co-author. In this way since 2005 [35], we have offered peers morphological and petrological details, so that we in the end hope to see the goal of understanding ikaite fully completed.

Conflicts of Interest: The authors declare no conflict of interest.

References

1. Schultz, B.P.; Thibault, N.; Huggett, J.M. The minerals ikaite and its pseudomorph glendonite: Historical perspective and legacies of Douglas Shearman and Alec, K. Smith. *Proc. Geol. Assoc.* **2022**, *133*, 176–192. [CrossRef]
2. Rogov, M.; Ershova, V.; Gaina, C.; Vereshchagin, O.; Vasileva, K.; Mikhailova, K.; Krylov, A. Glendonites throughout the Phanerozoic. *Earth-Sci. Rev.* **2023**, *241*, 104430. [CrossRef]
3. Schultz, B.P.; Vickers, M.L.; Huggett, J.; Madsen, H.; Heilmann-Clausen, C.; Friis, H.; Suess, E. Palaeogene glendonites from Denmark. Palaeogene glendonites from Denmark. *Bull. Geol. Soc. Den.* **2020**, *68*, 23–35. [CrossRef]
4. Schultz, B.P.; Huggett, J.M.; Kennedy, G.L.; Burger, P.; Jensen, A.M.; Kanstrup, M.; Bernasconi, S.M.; Thibault, N.; Ullmann, C.V.; Vickers, M.L.; et al. Petrography and geochemical analysis of Arctic ikaite pseudomorphs from Utqiagvik (Barrow), Alaska. *Nor. J. Geol.* **2023**, *103*, 202303. [CrossRef]
5. Schultz, B.P.; Huggett, J.; Ullmann, C.V.; Kassens, H.; Kölling, M. Links between Ikaite Morphology, Recrystallised Ikaite Petrography and Glendonite Pseudomorphs Determined from Polar and Deep-Sea Ikaite. *Minerals* **2023**, *13*, 841. [CrossRef]
6. Schultz, B.P.; Huggett, J.; Schootbrugge, B.V.D.; Ullmann, C.V.; Broch, M.C. Transgression Related Holocene Coastal Glendonites from Historic Sites. *Minerals* **2023**, *13*, 1159. [CrossRef]
7. Scheller, E.L.; Grotzinger, J.; Ingalls, M. Guttulatic calcite: A carbonate microtexture that reveals frigid formation conditions. *Geology* **2022**, *50*, 48–53. [CrossRef]
8. Frank, T.D.; Thomas, S.G.; Fielding, C.R. On using carbon and oxygen isotope data from glendonites as palaeoenvironmental proxies: A case study from the Permian system of eastern Australia. *J. Sediment. Res.* **2008**, *78*, 713–723. [CrossRef]
9. Swainson, I.P.; Hammond, R.P. Ikaite, CaCO3·6H2O: Cold comfort for glendonites as paleothermometers. *Am. Mineral.* **2001**, *86*, 1530–1533. [CrossRef]

10. Vickers, M.L.; Vickers, M.; Rickaby, R.E.; Wu, H.; Bernasconi, S.M.; Ullmann, C.V.; Bohrmann, G.; Spielhagen, R.F.; Kassens, H.; Schultz, B.P.; et al. The ikaite to calcite transformation: Implications for palaeoclimate studies. *Geochim. Cosmochim. Acta* **2022**, *334*, 201–216. [CrossRef]
11. Vickers, M.L.; Jones, M.T.; Longman, J.; Evans, D.; Ullmann, C.V.; Stokke, E.W.; Vickers, M.; Frieling, J.; Harper, D.T.; Clementi, V.J. IODP Expedition 396 Scientists: Paleocene-Eocene age glendonites from the Mid-Norwegian Margin—Indicators of cold snaps in the hothouse? *Clim. Past* **2024**, *20*, 1–23. [CrossRef]
12. Krylov, A.A.; Logvina, L.A.; Metveeva, T.M.; Prasolov, E.M.; Sapega, V.F.; Demedova, A.L.; Radchenko, M.S. Ikaite CaCO3·6H2O in bottom sediments of the Laptev Sea and the role of anaerobic methane oxidation in this mineral-forming process. *Proc. Russ. Mineral. Soc.* **2015**, *4*, 61–76.
13. Whiticar, M.J.; Suess, E.; Wefer, G.; Müller, P.J. Calcium Carbonate Hexahydrate (Ikaite): History of Mineral Formation as Recorded by Stable Isotopes. *Minerals* **2022**, *12*, 1627. [CrossRef]
14. Bohrmann, G.; Aromokeye, A.D.; Bihler, V.; Dehning, K.; Dohrmann, I.; Gentz, T.; Grahs, M.; Hogg, O.; Hüttich, D.; Kasten, S.; et al. *R/V METEOR Cruise Report M134, Emissions of Free Gas from Cross-shelf Troughs of South Georgia: Distribution, Quantification, and Sources for Methane Ebullition Sites in Sub-Antarctic Waters, Port Stanley (Falkland Islands)-Punta Arenas (Chile), 16 January–18 February 2017*; Berichte, MARUM—Zentrum für Marine Umweltwissenschaften, Fachbereich Geowissenschaften, Universität Bremen: Bremen, Germany, 2017; Volume 317, pp. 1–220. Available online: https://nbn-resolving.de/urn:nbn:de:gbv:46-00106081-12 (accessed on 23 February 2025).
15. Vickers, M.L.; Lengger, S.; Bernasconi, S.M.; Thibault, N.; Schultz, B.P.; Fernandez, A.; Ullmann, C.V.; McCormack, P.; Bjerrum, C.J.; Rasmussen, J.A.; et al. Cold spells in a Greenhouse world? The early Eocene glendonite paradox. *Nat. Commun.* **2020**, *11*, 4713. [CrossRef] [PubMed]
16. Kennedy, G.L.; Hopkins, D.M.; Pickthorn, W.J. Ikaite, the glendonite precursor, in estuarine sediments at Barrow, Arctic Alaska, Abstracts with Programs. *Geol. Soc. Am.* **1987**, *19*, 725.
17. Wefer, G.; Strasser, M.; Besuden, E.; Büttner, H.; Diekamp, V.; Dinten, D.; dos Santos Ferreira, C.; Fink, H.; Franke, P.; Fujiwara, T.; et al. *Report and Preliminary Results of R/V SONNE Cruise SO219A, Tohoku-Oki-Earthquake-Japan Trench, Yokohama-Yokohama, 8 March–6 April 2012*; Berichte, MARUM—Zentrum für Marine Umweltwissenschaften, Fachbereich Geowissenschaften, Universität Bremen: Bremen, Germany, 2012; pp. 1–83. Available online: http://publications.marum.de/id/eprint/2362 (accessed on 20 February 2025).
18. Greinert, J.; Derkachev, A. Glendonites and methane-derived Mg-calcites in the Sea of Okhotsk, Eastern Siberia: Implications of a venting-related ikaite/glendonite formation. *Mar. Geol.* **2004**, *204*, 129–144. [CrossRef]
19. Muramiya, Y.; Yoshida, H. A review of the occurrence and the origin of glendonite and glendonite concretion. *J. Geol. Soc. Jpn.* **2022**, *128*, 395–409. [CrossRef]
20. Geptner, A.R.; Vetoshkina, O.S.; Petrova, V.V. New data on the composition of stable isotopes in glendonites of the White Sea and their genesis. *Lithol. Miner. Resour.* **2014**, *49*, 473–490. [CrossRef]
21. Vasileva, K.; Zaretskaya, N.; Ershova, V.; Rogov, M.; Stockli, L.D.; Stockli, D.; Khaitov, V.; Maximov, F.; Chernyshova, I.; Soloshenko, N.; et al. New model for seasonal ikaite precipitation: Evidence from White Sea glendonites. *Mar. Geol.* **2022**, *449*, 106820. [CrossRef]
22. Gonzalez, C.R. Sobre la presencia de "glendonita" en el Paleozoico Superior de Patagonia. *Rev. Asoc. Geol. Argent.* **1980**, *35*, 417–420.
23. Steacy, H.R.; Grant, D.R. Tidal muds reveal mineral curiosity. *Can. Geogr. J.* **1974**, *88*, 36–38.
24. Qu, Q.; Teichert, B.M.A.; Birgel, D.; Goedert, J.L.; Peckmann, J. The prominent role of bacterial sulfate reduction in the formation of glendonite: A case study from Paleogene marine strata of western Washington State. *Facies* **2017**, *63*, 10. [CrossRef]
25. Freisleben, J.K. Uber einige interessante Vorkommnisse im Schlotztenleimen (Alluvialthon) bey Obersdorf, ohnweit Sangerhausen. *Isis Von Oken* **1827**, *20*, 334–337.
26. Counts, J.W.; Vickers, M.L.; Stokes, M.R.; Spivey, W.; Gardner, K.F.; Self-Trail, J.M.; Gooley, J.T.; McAleer, R.J.; Jubb, A.M.; Houseknecht, D.W.; et al. Insights into glendonite formation from the upper Oligocene Sagavanirktok Formation, North Slope, Alaska, USA. *J. Sediment. Res.* **2024**, *94*, 179–206. [CrossRef]
27. Suess, E.; Balzer, W.; Hesse, K.F.; Müller, P.J.; Ungerer, C.T.; Wefer, G. Calcium carbonate hexahydrate from organic-rich sediments of the Antarctic shelf: Precursors of glendonites. *Science* **1982**, *216*, 1128–1131. [CrossRef]
28. Brooks, R.; Clark, L.M.; Thurston, E.F. Calcium carbonate and its hydrates. *Philos. Trans. R. Soc. Lond.* **1950**, *243*, 145–167.
29. Buchardt, B.; Seaman, P.; Stockmann, G.; Vous, M.; Wilken, U.; Düwel, L.; Kristiansen, A.; Jenner, C.; Whiticar, M.J.; Kristensen, R.M.; et al. Submarine columns of ikaite tufa. *Nature* **1997**, *390*, 129–130. [CrossRef]
30. Zhou, X.; Lu, Z.; Rickaby, R.E.M.; Domack, E.W.; Wellner, J.S.; Kennedy, H.A. Ikaite abundance controlled by porewater phosphorus level: Potential links to dust and productivity. *J. Geol.* **2015**, *123*, 269–281. [CrossRef]
31. Purgstaller, B.; Dietzel, M.; Baldermann, A.; Mavromatis, V. Control of temperature and aqueous Mg2+/Ca2+ ratio on the (trans-) formation of ikaite. *Geochim. Cosmochim. Acta* **2017**, *217*, 128–143. [CrossRef]

32. Stockmann, G.; Tollefsen, E.; Skelton, A.; Brüchert, V.; Balic-Zunic, T.; Langhof, J.; Skogby, H.; Karlsson, A. Control of a Calcite inhibitor (phosphate) and Temperature on Ikaite precipitation in Ikka Fjord, Southwest Greenland. *Appl. Geochem.* **2018**, *89*, 11–22. [CrossRef]
33. Stockmann, G.J.; Seaman, P.; Balic-Zunic, T.; Peternell, M.; Sturkell, E.; Liljebladh, B.; Gyllencreutz, R. Mineral Changes to the Tufa Columns of Ikka Fjord, SW Greenland. *Minerals* **2022**, *12*, 1430. [CrossRef]
34. Tollefsen, E.; Balic-Zunic, T.; Morth, C.-M.; Bruchert, V.; Lee, C.C.; Skelton, A. Ikaite nucleation at 35 degrees C challenges the use of glendonite as a paleotemperature indicator. *Sci. Rep.* **2020**, *10*, 8141. [CrossRef]
35. Huggett, J.M.; Schultz, B.P.; Shearman, D.J.; Smith, A.J. The petrology of ikaite pseudomorphs and their diagenesis. *Proc. Geol. Assoc.* **2005**, *116*, 207–220. [CrossRef]
36. Stein, C.L.; Smith, A.J. *Authigenic Carbonate Nodules in the Nankai Trough, Site 583. Initial Reports of the Deep Sea Drilling Project, 77*; U.S. Government Printing Office: Washington, DC, USA, 1985; p. 668.
37. Bell, J.B.; Aquilina, A.; Woulds, C.; Glover, A.G.; Little, C.T.S.; Reid, W.D.K.; Hepburn, L.E.; Newton, J.; Mills, R.A. Geochemistry, faunal composition and trophic structure at an area of weak methane seepage on the southwest South Georgia margin. *R. Soc. Open Sci.* **2016**, *3*, 160284. [CrossRef]
38. Dana, E.S. A crystallographic study of the thinolite of Lake Lahontan. *United States Geol. Surv. Bull.* **1884**, *12*, 429–455.
39. Van Calker, F.J.P. XXIX. Beitrag zur Kenntniss des Pseudogaylussite und uber dessenVorkommen in Holland. P.Groth. *Z. Kryst. Mineral.* **1897**, *28*, 556–571.
40. MacNair, P. On pseudogaylussite dredged from the Clyde at Cardross and other recent additions to the Mineral Collections in the Kelvingrove Museum. *Proc. R. Philos. Soc. Glasg.* **1904**, *35*, 250–262.
41. Port, R.B. *Paleoclimate of the Late Oligocene Arctic Ocean: Molluscan Isotopic and Biotoc Evidence*; Florida Atlantic University: Boca Raton, FL, USA, 2008; pp. 1–214.
42. Selleck, B.; Carr, P.F.; Jones, B.G. A review and synthesis of glendonites (pseudomorphs after ikaite) with new data: Assessing applicability as recorders of ancient cold water conditions. *J. Sediment. Res.* **2007**, *77*, 980–991. [CrossRef]
43. Nesbitte, E.A.; Martin, R.A.; Campbell, K.A. New records of Oligocene diffuse hydrocarbon seeps, northern Cascadia margin. *Palaeogeogr. Palaeoclimatol. Palaeoecol.* **2013**, *390*, 116–129. [CrossRef]
44. Boggs, S. Petrography and geochemistry of rhombic calcite pseudomorphs from mid-Tertiary mudstone of the Pacific Northwest, USA. *Sedimentology* **1972**, *19*, 219–235. [CrossRef]
45. Brookes, I.A.; McAndrews, J.H.; von Bitter, P.H. Quaternary interglacial and associated deposits in southwest Newfoundland. *Can. J. Earth Sci.* **1982**, *19*, 410–423. [CrossRef]
46. David, T.W.E.; Taylor, T.G. Occurrence of pseudomorph glendonite in New South Wales, part 2. *Rec. New South Wales Geol. Surv.* **1905**, *8*, 162–179.
47. De Lurio, J.L.; Frakes, L.A. Glendonites as a paleoenvironmental tool: Implications for early Cretaceous high latitude climates in Australia. *Geochim. Cosmochim. Acta* **1999**, *633*, 1039–1048. [CrossRef]
48. Carr, P.; Southwood, M.; Jones, B.; Dowton, G. Opal Pineapples from White Cliffs New South Wales, Australia, Rocks and Minerals 2023, 98, 404–417. *Rocks Miner.* **2023**, *98*, 404–417. [CrossRef]
49. Carr, P.F.; Jones, B.G.; Middleton, R.G. Precursor and formation of glendonites in the Sydney Basin. *Aust. Mineral.* **1989**, *4*, 980–991.
50. Kaplan, M.E. Calcite pseudomorphs (pseudogaylussite, Jarrowite, Thinolite, Glendonite, Gennoishi, White Sea Hornlets) in Sedimentary Rocks. Origins of the pseudomorphs. *Litol. I Polezn. Iskop.* **1979**, *14*, 125–141. (In Russian)
51. Kemper, E. Das Klima der Kreide-Zeit. *Geols. Jahr.* **1987**, *96*, 185.
52. Grasby, S.; McCune, G.; Beauchamp, B.; Galloway, J. Lower Cretaceous cold snaps led to widespread glendonite occurrences in the Sverdrup Basin, Canadian High Arctic. *Geol. Soc. Am. Bull.* **2017**, *129*, 771–787. [CrossRef]
53. Mikhailova, K.; Rogov, M.; Ershova, V.; Vereshchagina, O.; Shurekovab, O.; Feodorovabc, A.; Zakharovb, V. Middle Jurassic–Lower Cretaceous glendonites from the eastern Barents Shelf as a tool for paleoenvironmental and paleoclimatic reconstructions. *Palaeogeogr. Palaeoclimatol. Palaeoecol.* **2021**, *579*, 110600. [CrossRef]
54. Spielhagen, R.F.; Tripati, A. Evidence from Svalbard for near-freezing temperatures and climate oscillations in the Arctic during the Paleocene and Eocene. *Palaeogeogr. Palaeoclimatol. Palaeoecol.* **2009**, *278*, 48–56. [CrossRef]
55. Vickers, M.; Watkinson, M.; Price, G.D.; Jerrett, R. An improved model for the ikaite glendonite transformation: Evidence from the Lower Cretaceous of Spitsbergen, Svalbard. *Nor. J. Geol.* **2018**, *98*, 1–15. [CrossRef]
56. Vasileva, K.; Rogov, M.; Ershova, V.; Mikhailova, K.; Vereshchagin, O.; Pokrovsky, B. Ikaite versus seep-related carbonate precipitation in the Late Jurassic–Early Cretaceous of West Spitsbergen: Evidence for cold versus warm climates? *Int. J. Earth Sci.* **2024**, *113*, 417–439. [CrossRef]
57. Vickers, M.L.; Jelby, M.E.; Blok, C.N.; Price, G.D.; Jerrett, R.M.; Jensen, M.A.; Jones, M.T. Early Cretaceous giant glendonites: A record of (sub-)millennial-scale cooling? *Palaeogeogr. Palaeoclimatol. Palaeoecol.* **2025**, *661*, 112739. [CrossRef]
58. Teichert, B.M.A.; Luppold, F.W. Glendonites from an Early Jurassic methane seep—Climate or methane indicators? *Palaeogeogr. Palaeoclimatol. Palaeoecol.* **2013**, *390*, 81–93. [CrossRef]

59. Rogov, M.; Ershova, V.; Vereshchagin, O.; Vasileva, K.; Mikhailova, K.; Krylov, A. Database of global glendonite and ikaite records throughout the Phanerozoic. *Earth Syst. Sci. Data* **2021**, *13*, 343–356. [CrossRef]
60. Kennedy, G.L. Glendonites: Enigmatic mineral pseudomorphs and their ephemeral precursor. *Rocks Min.* **2022**, *97*, 496–508. [CrossRef]
61. Viola, C. XXX. Über Aetzfiguren am Gyps. *Z. Kryst. Mineral.* **1897**, *28*, 573–578.
62. Goldschmidt, V. *Atlas der Krystallformen*; Winter: Heidelberg, Germany, 1913.
63. Goldschmidt, V.M. Entwicklung d. Krystallformen II, Taf VIII & IX. *Z. Kryst. Mineral.* **1923**, *28*, 414–451.
64. Hintze, C. Nitrate, Jodate, Karbonate, Selenite, Tellurite, Manganite, Plumbate. In *Handbuch der Mineralogie, Veit & Comp*; Der Verlag Walter de Gruyter & Co.: Berlin, Germany, 1915; pp. 2790–2802+3650.
65. Blum, J.R. *Pseudomorphosen*; dritter Nachtrag, p. 13.; 1863; vierter Nachtrag p. 8, l879.
66. Ito, T. Ikaite from cold spring water at Shiowakka, Japan. *J. Econ. Mineral. Petrol.* **1996**, *91*, 209–219. [CrossRef]
67. Friedel, G. *Leçons de Cristallographie Profèssés à la Faculté des Sciences de Strasbourg*; Berger-Levrault: Paris, France, 1926; 602p.
68. Shearman, D.J.; Smith, A.J. Ikaite, the parent mineral of jarrowite-type pseudomorphs. *Proc. Geol. Assoc.* **1985**, *96*, 305–314. [CrossRef]
69. Mitterer, R.M.; Cunningham, R., Jr. The interaction of natural organic matter with grain surfaces: Implications for calcium carbonate precipitation. *Soc. Econ. Paleontol. Mineral.* **1985**, *36*. [CrossRef]
70. Raven, M.J.; Dickson, J.A.D. Fir-tree zoning: An indicator of pulsed crystallization in calcite cement crystals. *Sediment. Geol.* **1989**, *65*, 249–259. [CrossRef]
71. Pedersen, G.K.; Surlyk, F. The Fur Formation, a late Paleocene ash-bearing diatomite from northern Denmark. *Bull. Geol. Soc. Den.* **1983**, *32*, 43–65. [CrossRef]
72. Schoon, P.L.; Heilmann-Clausen, C.; Schultz, B.P.; Sluijs, A.; Sinninghe Damsté, J.S.; Schouten, S. Recognition of Early Eocene global carbon isotope excursions using lipids of marine Thaumarchaeota. *Earth Planet. Sci. Lett.* **2013**, *373*, 60–168. [CrossRef]
73. Stokke, E.W.; Jones, M.T.; Tierney, J.E.; Svensen, H.H.; Whiteside, J.H. Temperature changes across the Paleocene-Eocene Thermal Maximum—A new high-resolution TEX86 temperature record from the Eastern North Sea Basin. *Earth Planet. Sci. Lett.* **2020**, *544*, 116388. [CrossRef]
74. Stokke, E.W.; Jones, M.T.; Riber, L.; Haflidason, H.; Midtkandal, I.; Schultz, B.P.; Svensen, H.H. Rapid and sustained environmental responses to global warming: The Paleocene–Eocene Thermal Maximum in the eastern North Sea. *Clim. Past* **2021**, *17*, 1989–2013. [CrossRef]
75. Jones, M.T.; Percival, L.M.E.; Stokke, E.W.; Frieling, J.; Mather, T.A.; Riber, L.; Schubert, B.A.; Schultz, B.; Tegner, C.; Planke, S.; et al. Mercury anomalies across the Palaeocene-Eocene Thermal Maximum. *Clim. Past* **2019**, *15*, 217–236. [CrossRef]
76. Jones, M.T.; Stokke, E.W.; Rooney, A.D.; Frieling, J.; Pogge von Strandmann, P.A.E.; Wilson, D.J.; Svensen, H.H.; Planke, S.; Adatte, T.; Thibault, N.; et al. Tracing North Atlantic volcanism and seaway connectivity across the Paleocene–Eocene Thermal Maximum (PETM). *Clim. Past* **2023**, *19*, 1623–1652. [CrossRef]
77. Turner, S.K. Constraints on the onset duration of the paleocene–eocene thermal maximum. Philosophical Transactions of the Royal Society. *Math. Phys. Eng. Sci.* **2018**, *376*, 20170082. [CrossRef]
78. Baumann, N.B.; Regelous, M.; Adatte, T.; Thibault, N.R.; Regelous, A.; Schultz, B.P.; Fantasia, A.; Madsen, H.; Haase, K.M. Linking the PETM and North Atlantic volcanism using tellurium in sediments. *Palaeogeogr. Palaeoclimatol. Palaeoecol.* **2024**, *656*, 112575. [CrossRef]
79. Heingård, M.; Sjövall, P.; Sylvestersen, R.L.; Schultz, B.P.; Lindgren, J. Crypsis in the pelagic realm: Evidence from exceptionally preserved fossil fish larvae from the Eocene Stolleklint Clay of Denmark. *Palaeontology* **2021**, *64*, 805–815. [CrossRef]
80. Heingård, M.; Sjövall, P.; Schultz, B.P.; Sylvestersen, R.L.; Lindgren, J. Preservation and Taphonomy of Fossil Insects from the Earliest Eocene of Denmark. *Biology* **2022**, *11*, 395. [CrossRef]
81. Lindgren, J.; Uvdal, P.; Sjövall, P.; Nilsson, D.E.; Schultz, B.P.; Theil, V. Molecular preservation of the pigment melamin in fossil melanosomes. *Nat. Commun.* **2012**, *3*, 824. [CrossRef]
82. Lindgren, J.; Sjövall, P.; Carney, R.M.; Uvdal, P.; Gren, J.A.; Dyke, G.; Schultz, B.P.; Shawkey, M.D.; Barnes, K.R.; Polcyn, M.J. Skin pigmentation provides evidence of convergent melanism in extinct marine reptiles. *Nature* **2014**, *506*, 484–488. [CrossRef] [PubMed]
83. Lindgren, J.; Moyer, A.; Higby Schweitzer, M.; Sjövall, P.; Uvdal, P.; Nilsson, D.-E.; Heimdal, J.; Engdahl, A.; Gren, J.; Schultz, B.P.; et al. Interpreting melanin-based coloration through deep time: A critical review. Royal Society of London. *Proc. B Biol. Sci.* **2015**, *282*, 20150614. [CrossRef]
84. Lindgren, J.; Nilsson, D.; Sjövall, P.; Jarenmark, M.; Ito, S.; Wakamatsu, K.; Kear, B.P.; Schultz, B.P.; Sylvestersen, R.L.; Madsen, H.; et al. Fossil insect eyes shed light on trilobite optics and the arthropod pigment screen. *Nature* **2019**, *573*, 122–125. [CrossRef] [PubMed]

85. Simonsen, T.J.; Sylvestersen, R.L.; Olsen, K.; Rasmussen, J.A. Apachyus madseni (Dermaptera: Apachyidae) sp. nov. from the Ypresian Fur Formation of Denmark: The first fossil record of the enigmatic earwig family Apachyidae. *Palaeoentomology* **2024**, *7*, 638–644. [CrossRef]
86. Schroeder, A.; Carnevale, G. The argentiniform Surlykus longigracilis gen. et sp. nov.; the most abundant fish from the Eocene Fur Formation of Denmark. *Bull. Geol. Soc. Den.* **2024**, *72*, 1–18. [CrossRef]
87. Nenning, F. Mega-Glendonites in the Early Eocene Fur Formation: Unraveling Paleoenvironmental Conditions in the Danish Basin and Their Influence on Glendonite Formation. 2017. Available online: https://nbn-resolving.de/urn:nbn:de:hbz:6-51229483616 (accessed on 20 February 2025).
88. Larsen, L.M.; Fitton, J.G.; Pedersen, A.K. Paleogene volcanic ash layers in the Danish Basin: Compositions and source areas in the North Atlantic Igneous Province. *Lithos* **2003**, *71*, 47–80. [CrossRef]
89. Heilmann-Oausen, C.; Nielsen, O.B.; Gersner, P. Lithostratigraphy and depositional environments in the Upper Paleocene and Eocene of Denmark. *Bull. Geol. Soc. Den.* **1985**, *33*, 287–323. [CrossRef]
90. Rasmussen, J.A.; Madsen, H.; Schultz, B.P.; Sylvestersen, R.L.; Bonde, N. The lowermost Eocene deposits and biota of the western Limfjord region, Denmark—Field Trip Guidebook. In Proceedings of the 2nd International Mo-Clay Meeting, Nykøbing Mors, Denmark, 2–4 November 2016; p. 35.
91. Pedersen, G.K.; Pedersen, S.A.S.; Bonde, N.; Heilman-Clausen, C.; Larsen, L.M.; Lindow, B.; Madsen, H.; Pedersen, A.K.; Rust, J.; Schultz, B.P.; et al. Moleområdets geologi—Sedimenter, fossiler, askelag og glacialtektonik. In *Geologisk Tidsskrift*; Dansk Geologisk Forening: Copenhagen, Denmark, 2011; pp. 41–135. Available online: https://2dgf.dk/wp-content/uploads/2016/05/gt2011-41-135.pdf (accessed on 23 February 2025).
92. Pedersen, G.K.; Buchardt, B. The calcareous concretions (cementsten) in the Fur Formation (Paleogene, Denmark). Isotopic evidence of early diagenetic growth. *Bull. Geol. Soc. Den.* **1996**, *43*, 78–86. [CrossRef]
93. McNamara, M.E.; Briggs, D.E.G.; Orr, P.J.; Field, D.J.; Wang, Z. Experimental maturation of feathers: Implications for reconstructions of fossil feather colour. *Biol. Lett.* **2013**, *9*, 20130184. [CrossRef] [PubMed]
94. Stockmann, G.J.; Ranta, E.; Trampe, E.; Sturkell, E.; Seaman, P. Carbon mineral storage in seawater: Ikaite (CaCO3·6H2O) columns in Greenland. *Energy Procedia* **2018**, *146*, 59–67. [CrossRef]
95. Carmiggelt, J.; King, H.; Wolthers, M.; Schulz, B.P.; Van de Schootbrugge, B. Promotion of ikaite precipitation by bentonite fertilisation in the Eocene Fur formation, northern Denmark. In Proceedings of the EGU General Assembly 2023, Vienna, Austria, 24–28 April 2023. [CrossRef]
96. Mikkelsen, A.; Andersen, A.B.; Engelsen, S.B.; Hansen, H.C.B.; Larsen, O.; Skibsted, L.H. Presence and dehydration of ikaite, calcium carbonate hexahydrate, in frozen shrimp shell. *J. Agric. Food Chem.* **1999**, *47*, 911–917. [CrossRef] [PubMed]
97. Carr, P.; Jones, B.G.; Selleck, B. The Sydney Basin and Frozen Prawns—The Cool Mineral Connection. 2006. Available online: https://ro.uow.edu.au/scipapers/4837 (accessed on 20 February 2025).
98. Tansman, G.; Kindstedt, P.; Hughes, J. Minerals in Food: Crystal Structures of Ikaite and Struvite from Bacterial Smears on Washed-Rind Cheese. *Can. Mineral.* **2017**, *55*, 89–100. [CrossRef]
99. Garvie, L.A.J. Seasonal formation of ikaite in slime flux jelly on an infected tree (Populus fremontii) wound from the Sonoran Desert. *Sci Nat.* **2022**, *109*, 48. [CrossRef]
100. Milodowski, A.; Shaw, R.; Stewart, D. *The Harpur Hill Site: Its Geology, Evolutionary History and a Catalogue of Materials Present. CR/13/104*; British Geological Survey: Nottingham, UK, 2013; 43p.
101. Shaikh, A.M. A new crystal growth form for vaterite, CaCO3. *J. Appl. Crystallogr.* **1990**, *23*, 263–265. [CrossRef]
102. Zabel, M.; Schulz, H.D. Importance of submarine landslides for non-steady state conditions in pore water systems-lower Zaire (Congo) deep-sea fan. *Mar. Geol.* **2001**, *176*, 87–99. [CrossRef]
103. Nielsen, T.; Laier, T.; Kuijpers, A.; Rasmussen, T.; Mikkelsen, N.; Nørgaard-Pedersen, N. Fluid flow and methane occurrences in the Disko Bugt area offshore West Greenland: Indications for gas hydrates? *Geo-Mar. Lett.* **2014**, *34*, 511–523. [CrossRef]
104. Kodina, L.A.; Tokarev, V.G.; Vasova, L.N.; Korobeinik, G.S. Contribution of biogenic methane to ikaite formation in the Kara Sea: Evidence from the Stable Carbon Isotope Geochemistry. In *Siberian River Run-Off in the Kara Sea: Characterisation, Quantification, Variability, and Environmental Significance*; Stein, R., Fahl, K., Fütterer, D.K., Galimov, E.M., Stepanets, O.V., Eds.; Elsevier: Amsterdam, The Netherlands, 2003; pp. 349–375.
105. Bornhold, B.D.; Firth, J.V.; Adamson, L.M.; Baldauf, J.G.; Blais, A.P.; Elvert, M.; Fox, P.J.; Hebda, R.; Kemp, A.E.S.; Mora, K.; et al. Sites 1033 and 1034. *Proc. Ocean. Drill. Program Initial. Rep.* **1998**, *27*, 11–61. Available online: http://www-odp.tamu.edu/publications/169S_IR/PRELIM.PDF (accessed on 20 February 2025).
106. Kassen, H.; Dmitrenko, I. The TRANSDRIFT II Expedition to the Laptev Sea Reports on Polar Research, Laptev Sea Systems Expedition Beretten. *Polarforsch* **1994**, *182*, 93.
107. Lu, Z.; Rickaby, R.E.M.; Kennedy, H.; Kennedy, P.; Pancost, R.D.; Shaw, S.; Lennie, A.; Wellner, J.; Anderson, J.B. An ikaite record of late Holocene climate at the Antartic Peninsula. *Earth Planet. Sci. Lett.* **2012**, *325*, 108–115. [CrossRef]

108. Rysgaard, S.; Glud, R.N.; Lennert, K.; Cooper, M.; Halden, N.; Leakey, R.J.G.; Hawthorne, F.C.; Barber, D. Ikaite crystals in melting sea ice—Implications for pCO2 and pH levels in Arctic surface waters. *Cryosphere* **2012**, *6*, 901–908. [CrossRef]
109. Dieckmann, G.S.; Nehrke, G.; Papadimitriou, S.; Gottlicher, J.; Steininger, R.; Kennedy, H.; Wolf-Gladrow, D.; Thomas, D.N. Calcium carbonate as ikaite crystals in Antarctic sea ice. *Geophys. Res. Lett.* **2008**, *35*, 1–3. [CrossRef]
110. Pauly, H. Ikaite, a New Mineral from Greenland. *Arctic* **1963**, *16*, 213–292. [CrossRef]
111. Bischoff, J.L.; Stine, S.; Rosenbauer, R.J.; Fitzpatrick, J.A.; Stafford, T.W. Ikaite precipitation by mixing of shoreline springs and lake water, Mono Lake, California, USA. *Geochim. Cosmochim. Acta* **1993**, *57*, 3855–3866. [CrossRef]
112. Last, F.M.; Last, W.M.; Fayek, M.; Halden, N. Occurrence and significance of a coldwater carbonate pseudomorph in microbialites from a saline lake. *J. Paleolimnol.* **2013**, *50*, 505–517. [CrossRef]
113. Pollard, W.; Omelon, C.; Andersen, D.; McKay, C. Perennial spring occurrence in the Expedition Fiord area of western Axel Heiberg Island, Canadian High Arctic. *Can. J. Earth Sci.* **1999**, *36*, 105–120. [CrossRef]
114. Ohlendorf, C.; Fey, M.; Massaferro, J.; Haberzettl, T.; Laprida, C.; Lücke, A.; Maidana, N.; Mayr, C.; Oehlerich, M.; Ramón, M.J.; et al. Late Holocene hydrology inferred from lacustrine sediments of Laguna Cháltel (southeastern Argentina). *Palaeogeogr. Palaeoclimatol. Palaeoecol.* **2014**, *411*, 229–248. [CrossRef]
115. Nèmeth, P.; Toechterle, P.; Dublyansky, Y.; Stalder, R.; Molnár, Z.; Klébert, S.; Spötl, C. Tracing structural relicts of the ikaite-to-calcite transformation in cryogenic cave glendonite. *Am. Mineral.* **2022**, *10*, 1960–1967. [CrossRef]
116. Marland, G.H. The stability of CaCO3·6H2O (ikaite). *Geochim. Cosmochim. Acta* **1975**, *39*, 83–91. [CrossRef]
117. Hu, Y.-B.; Wolf-Gladrow, D.A.; Dieckmann, G.S.; Völker, C.; Nehrke, G. A laboratory study of ikaite (CaCO3·6H2O) precipitation as a function of pH, salinity, temperature and phosphate concentration. *Mar. Chem.* **2014**, *162*, 10–18. [CrossRef]
118. Lázár, A.; Molnár, Z.; Demény, A.; Kótai, L.; Trif, L.; Béres, K.; Bódis, E.; Bortel, G.; Aradi, L.; Karlik, M.; et al. Insights into the amorphous calcium carbonate (ACC) → ikaite → calcite transformations. *Cryst. Eng. Comm.* **2022**, *25*, 738–750. [CrossRef]
119. Tollefsen, E.; Stockmann, G.; Skelton, A.; Mörth, C.M.; Dupraz, C.; Sturkell, E. Chemical controls on ikaite formation. *Mineral. Mag.* **2018**, *82*, 1–22. [CrossRef]
120. Slack, J.G. Calcium carbonate hexahydrate: Its properties and formation in lime-soda softening. *Water Res.* **1980**, *14*, 799–804. [CrossRef]
121. Boch, R.; Dietzel, M.; Reichl, P.; Leis, A.; Baldermann, A.; Mittermayr, F.; Poelt, P. Rapid ikaite (CaCO3·6H2O) crystallization in a man-made river bed: Hydrogeochemical monitoring of a rarely documented mineral formation. *Appl. Geochem.* **2015**, *63*, 366–379. [CrossRef]
122. Field, L.P.; Milodowski, A.E.; Shaw, R.P.; Stevens, L.A.; Hall, M.R.; Kilpatrick, A.; Gunn, J.; Kemp, S.J.; Ellis, M.A. Unusual morphologies and the occurrence of pseudomorphs after ikaite (CaCO3·6H2O) in fast growing, hyperalkaline speleothems. *Mineral. Mag.* **2017**, *81*, 565–589. [CrossRef]
123. Bastianini, L.; Rogerson, M.; Brasier, A.; Prior, T.J.; Hardman, K.; Dempsey, E.; Bird, A.; Mayes, W.M. Ikaite formation in streams affected by steel waste leachate: First report and potential impact on contaminant dynamics. *Chem. Geol.* **2023**, *644*, 121842. [CrossRef]
124. Németh, P. Diffraction Features from (101¯4) Calcite Twins Mimicking Crystallographic Ordering. *Minerals* **2021**, *11*, 720. [CrossRef]
125. Vasileva, K.; Ershova, V.; Rogov, M.; Gritsenko, Y.; Maximov, F.; Ovsepyan, Y.; Okuneva, T.; Rybakova, A.; Kiseleva, D.; Vereshchagin, O. Mineralogical composition, isotopic and geochemical characteristics of Pleistocene glendonites from the outcrops of Bol'shaya Balakhnya River, Eastern Taimyr, Russia. *J. Sediment. Res.* **2024**, *94*, 355–366. [CrossRef]
126. Oenema, S. *Pseudogaylussiet in Het Nederlandse en Duitse Kustgebied*; Grondboor en Hamer: München, Germany, 1990; p. 163.
127. Trechmann, C.O. Uber einen Fund von ausgezeichneten Pseudogaylussite (Thinolite Jarrowite -) Krystallen. *Z. Kryst.* **1901**, *25*, 283–285.

Disclaimer/Publisher's Note: The statements, opinions and data contained in all publications are solely those of the individual author(s) and contributor(s) and not of MDPI and/or the editor(s). MDPI and/or the editor(s) disclaim responsibility for any injury to people or property resulting from any ideas, methods, instructions or products referred to in the content.